This is a repository copy of *A γδ T cell-IL-3 axis controls allergic responses through sensory neurons*.

Version: Accepted Version

Article:

A γδ T cell-IL-3 axis controls allergic responses through sensory neurons

Cameron H Flayer, Ph.D.[1], Isabela J Kernin, M.S.[1,±], Peri Matatia[1,2,±], Xiangsunze Zeng, Ph.D.[3], David A Yarmolinsky, Ph.D.[3], Cai Han, Ph.D.[1], Parth R Naik, M.S.[1], Dean R Buttaci[1], Pamela A Aderhold[1], Ryan B Camire[2], Xueping Zhu, Ph.D.[1], Alice J Tirard[1], John T McGuire[1], Neal P Smith, M.S.[1], Clive S McKimmie, Ph.D.[4], Cameron S McAlpine, Ph.D.[5,6], Filip K Swirski, Ph.D.[5], Clifford J Woolf, M.B.,B.Ch, Ph.D.[3], Alexandra-Chloe Villani, Ph.D.[1], Caroline L Sokol, M.D., Ph.D.[1,2,*]

[1]Massachusetts General Hospital, Harvard Medical School, MA, USA

[2]Department of Immunology, Harvard Medical School, Boston, MA 02155, USA

[3]FM Kirby Center, Boston Children's Hospital and Department of Neurobiology, Harvard Medical School, MA, USA

[4]Virus Host Interaction Team, Skin Research Centre, University of York, York, YO10 5DD, UK

[5]Cardiovascular Research Institute and the Department of Medicine, Cardiology, Icahn School of Medicine at Mount Sinai, NY, USA

[6]Friedman Brain Institute and the Nash Family Department of Neuroscience, Icahn School of Medicine at Mount Sinai, NY, USA

Summary

In naïve individuals, sensory neurons directly detect and respond to allergens, leading both to the sensation of itch and the activation of local innate immune cells, which initiate the allergic immune response[1,2]. In the setting of chronic allergic inflammation, immune factors

[*]Corresponding author Caroline L Sokol, M.D., Ph.D. (clsokol@mgh.harvard.edu).
[±]These authors contributed equally

prime sensory neurons, causing pathologic itch[3–7]. While these bidirectional neuroimmune circuits drive responses to allergens, whether immune cells regulate the set-point for neuronal activation by allergens in the naïve state is unknown. Here we describe a γδ T cell-IL-3 signaling axis that controls the allergen responsiveness of cutaneous sensory neurons. We define a poorly characterized epidermal γδ T cell subset[8], termed GD3 cells, that produces its hallmark cytokine IL-3 to promote allergic itch and the initiation of the allergic immune response. Mechanistically, IL-3 acts on *Il3ra*-expressing sensory neurons in a JAK2-dependent manner to lower their threshold for allergen activation without independently eliciting itch. This γδ T cell-IL-3 signaling axis further acts via STAT5 to promote neuropeptide production and the initiation of allergic immunity. These results reveal an endogenous immune rheostat that sits upstream of and governs sensory neuronal responses to allergens upon first exposure. This pathway may explain individual differences in allergic susceptibility and opens novel therapeutic avenues for treating allergic diseases.

Sensory neurons densely innervate the skin and respond to inflammatory, pathogenic, and allergic triggers that direct downstream immune responses[1,2,9–11]. Allergens activate sensory neurons directly through their enzymatic activity, leading to the sensation of itch and the release of neuropeptides at the site of allergen exposure[1,2]. Sensory neuronal activation leads to the migration of mature, allergen-bearing dendritic cells (DCs) from the periphery to draining lymph nodes (dLN), where they initiate Th2 differentiation and allergic sensitization[1,12]. In the setting of chronic allergen exposure, these Th2 cells, as well as other inflammatory cells, can traffic back to the skin, releasing immune factors that activate or alter the responsiveness of sensory neurons. The allergic factors TSLP[3], LTC$_4$[4,5], and IL-31[6] directly elicit itch and scratching, while IL-4 and IL-13 prime sensory neurons[7], lowering their threshold for activation by other pruritogens without independently causing itch. However, in the absence of allergic inflammation or in naïve skin, whether the immune system plays a role in establishing the primary "set-point" for neuronal activation by allergens is unknown. We hypothesized that a cutaneous innate immune cell and its production of a priming factor controls the allergen activation of sensory neurons upon their first exposure to an allergen, governing itch and the initiation of allergic immunity. We identify a poorly characterized epidermal γδ T cell population, which we term GD3 cells, that produces IL-3 under homeostatic conditions and tunes the responsiveness of *Il3ra*-expressing sensory neurons to allergens through distinct JAK2 and STAT5-dependent effects. This γδ T cell-IL-3 axis sits upstream of and regulates the initial sensory neuronal response to allergens, constituting a novel pathway for the innate immune control of allergic itch and allergen sensitization.

γδ T cells promote allergen-induced itch

Using the itch and scratch response to the model allergen papain in naïve mice as a readout of allergen activation of sensory neurons[1,13,14], we performed a behavioral screen of mice genetically deficient in specific immune cell populations, none of which displayed spontaneous nonspecific itch behavior (Extended Data Fig. 1a–b). Despite well-characterized roles in IgE and MRGPR-mediated itch[5,15], mast cell or basophil deficiency had no effect on papain-induced scratching (Extended Data Fig. 1c). Instead, papain-induced

itch was defective in lymphocyte (*Rag2*^{-/-}) and $\gamma\delta$ T cell-deficient (*Tcrd*^{-/-}) mice, but intact in mice deficient in B or $\alpha\beta$ T cells (Figure 1a). The effect of $\gamma\delta$ T cell deficiency on itch was shared among diverse allergens, including extracts of house dust mite (HDM), *Alternaria*, fire ant, and mosquito saliva (Figure 1b). Itch to histamine or chloroquine and pain to capsaicin were intact in *Tcrd*^{-/-} mice (Extended Data Fig. 1d–e), and there was no difference in cutaneous innervation between WT and *Tcrd*^{-/-} mice (Extended Data Fig. 1f). These data indicate that while $\gamma\delta$ T cells are required for allergen-induced itch, their absence does not cause broad defects in sensory neuronal function or innervation.

The axons of peripheral sensory neurons extend from their cell bodies in the dorsal root ganglia (DRG) to the skin. $\gamma\delta$ T cells (live CD45^{+}Lineage^{−}CD3^{+}TCR$\gamma\delta$[+]) were detected in the skin, but not the DRG (Extended Data Fig. 2a–b). Two populations of $\gamma\delta$ T cells with distinct TCR rearrangement and effector function seed the dermis and epidermis[8]: dermal $\gamma\delta$ T cells are TCR$\gamma\delta$[intermediate], while dendritic epidermal T cells (DETCs) are Vγ5[+] and TCR$\gamma\delta$[high]. Flow cytometry of naïve WT mouse skin confirmed the presence of these stereotypical populations and identified an additional Vγ5[−]TCR$\gamma\delta$[high] epidermal subset (Figure 1c; Extended Data Fig. 2c–d), which we termed GD3 cells. The frequency of these $\gamma\delta$ T cell populations, including GD3 cells, was unaffected by chronic allergic inflammation (Extended Data Fig. 2e–g), so we focused our efforts on understanding exactly how these innate immune cells control the sensory neuronal response to initial allergen exposure in naïve skin.

$\gamma\delta$ T cells are important in the development and homeostasis of immune cells and tissues[16]. To rule out off-target effects from the constitutive loss of $\gamma\delta$ T cells, we inducibly depleted cutaneous $\gamma\delta$ T cells in *Tcrd*[GDL] and *iTcrd*[DTA] mice, which reduced papain-induced itch (Figure 1d–e; Extended Data Fig. 3a–d). Epidermal DETCs and GD3 cells were preferentially depleted *iTcrd*[DTA] mice, suggesting that epidermal, but not dermal $\gamma\delta$ T cells, are required for allergic itch. To assess the role of DETCs in allergic itch, we examined FVB/N mice deficient in DETCs due to a spontaneous point mutation in the *Skint1* gene[17]. Compared to *Skint1*^{+/+} (FVB/N-Jax) controls, *Skint1*^{−/−} (FVB/N-Tac) mice lacked DETCs, which were largely replaced by GD3 cells(Figure 1f; Extended Data Fig. 3e). Despite a deficiency in DETCs, *Skint1*^{−/−} mice had no defect in papain, HDM, histamine, or chloroquine-induced itch (Figure 1g; Extended Data Fig. 3f).

With our data suggesting a limited role for dermal $\gamma\delta$ T cells and DETCs in establishing the allergen responsiveness of sensory neurons, we asked if GD3 cells control this pathway through a secreted factor. Stimulated GD3-cell supernatant, but not dermal $\gamma\delta$ T cell, DETC, or cell-free supernatant, enhanced papain-induced itch (Figure 1h–i; Extended Data Fig. 3g). These data suggest that GD3 cells produce a secreted factor that tunes the sensory neuronal response to a primary allergen exposure.

GD3 cells are a unique $\gamma\delta$ T cell subset

Despite previous visualization of Vγ5[−] epidermal $\gamma\delta$ T cells[18–20], they have never been characterized. To determine the transcriptional signature of GD3 cells, we performed single-cell RNA (scRNAseq) and TCR$\gamma\delta$ (scTCRseq) sequencing on FACS-isolated cutaneous

γδ T cells. Pooled transcriptomic analysis revealed that GD3 cells were transcriptionally distinct from dermal γδ T cells and DETCs (Figure 2a). As expected, we identified Vγ4⁺ (*Trgv4*) and Vγ6⁺ (*Trgv6*) dermal γδ T cells and Vγ5⁺ (*Trgv5*) DETCs[18,21,22], while Vγ4 (*Trgv4*) primarily characterized GD3 cells (Supplementary Fig. 1a). Compared to highly clonal DETCs (n=285 clones), oligoclonal GD3 cells (n=948 clones) exhibited more diversity, with the *Trgv4-Trdv2–2* pairing being the dominant clonotype (Figure 2b; Supplementary Fig. 1b). Flow cytometry validated that the majority of GD3 cells were marked by Vγ4, often paired with Vδ4 (*Trdv2–2*), with a smaller population of Vγ7⁺ cells absent of Vδ4 (Figure 2c; Supplementary Fig. 1c–d). Nonetheless, TCR usage did not define transcriptionally independent subsets of GD3 cells (Supplementary Fig. 2a); rather, RNA velocity identified a gene expression program gradient (Supplementary Fig. 2b–c). Transcriptional analysis suggested that GD3 cells have higher expression of *Ly6a* (Sca-1) and lower expression of *Il18r1* (IL-18Rα; compared to DETCs and dermal γδ T cells) and *Cd9* (CD9; compared to DETCs), which we validated with flow cytometry (Supplementary Fig. 2d–f). *Trgv4* deficiency led to an absence of Vγ4⁺ GD3 cells and phenocopied the papain-induced itch defect in *Tcrd⁻/⁻* mice (Figure 2d; Extended Data Fig. 4a). These data indicate that GD3 cells are a *bona fide* cutaneous γδ T cell subset and that the dominant Vγ4⁺ clones promote allergen activation of sensory neurons.

Aging alters the epidermal compartment[23] and was associated with reduced GD3 cell numbers (Extended Data Fig. 4b). Commensal microbes regulate cutaneous immune cells, including dermal γδ T cells[24]. Dermal γδ T cells, GD3 cells, and allergic itch were deficient in germ-free (GF) mice (Extended Data Fig. 4c–d). Reintroduction of commensal microbiota into adult mice by co-housing SPF with GF mice (exSPF and exGF) restored GD3 cell numbers (Extended Data Fig. 4e). GD3 cells were detected in genetically diverse and microbially rich pet shop mice (Extended Data Fig. 4f). Given the positive association between dry skin and allergic sensitization[25,26], we hypothesized that GD3 cells accumulate in dry skin. Indeed, GD3 cells increased in the skin of WT mice treated with acetone:diethylether and water (AEW) compared to sham controls, even in the absence of CD45⁺ immune cell infiltration (Extended Data Fig. 4g–h). Together, these data suggest that physiologic and environmental factors control GD3 cell numbers.

The epidermis is a thin epithelium that must balance its role in sensing the external environment through innervation by free nerve endings with that as a physical barrier. Confocal immunofluorescence microscopy of epidermal sheets showed that Vδ4⁺ GD3 cells (of the dominant Vγ4⁺Vδ4⁺ GD3 clonotype) were found in clusters adjacent to DETCs and mirrored their hallmark dendritic morphology[20,27] (Supplementary Fig. 3a). The presence of GD3 cell clusters is consistent with local proliferative units and clonal self-renewal, as previously observed in Vγ5⁺ DETCs[27]. Vδ4⁺ GD3 cells and DETCs formed direct contacts with *Scn10a^tdTomato* (Nav1.8⁺) nociceptive and pruriceptive free nerve endings (Figure 2e–f; Supplementary Fig. 3b), demonstrating the intimate association and neuroimmune network formation between epidermal γδ T cells and sensory neurons.

Through multiple in-frame premature termination codons, humans are functionally devoid of *Skint1*[28], suggesting there is no direct human equivalent to mouse Vγ5⁺ DETCs[16]. Given the comparable lack of *Skint1* between humans and *Skint1⁻/⁻* (FVB/N-Tac) mice that

contain abundant GD3 cells, we compared mouse GD3 cells to human epidermal cells using the Gellatly et al.[29] scRNAseq dataset. Mouse GD3 cells showed significant transcriptional similarity to human αβ and γδ T cells, though we also detected statistically significant similarities between mouse GD3 cells and human melanocytes (Figure 2g–j; Supplementary Fig. 4a). An analogous comparison of mouse GD3 cells to normal human cutaneous T and innate lymphoid cells (ILCs) from Reynolds et al.[30] revealed that the populations with the highest normalized enrichment scores were NK cells and γδ T cells (Supplementary Fig. 4b–e). Despite differences in the sequencing methods and isolation protocols used among the datasets, in both cases, mouse GD3 cells shared a common transcriptional signature with human γδ T cells in normal skin.

Allergic itch requires GD3-derived IL-3

Our data indicate that a GD3 cell-secreted factor heightens the allergen responsiveness of sensory neurons (Figure 1i). A multiplex assay with validation by ELISA revealed that the only unique factor secreted by αCD3/CD28-stimulated GD3 cells was IL-3, while dermal γδ T cells produced IL-17A (Figure 3a; Extended Data Fig. 5a–b). Vγ4$^+$ GD3 cells produced significantly more IL-3 than Vγ7$^+$ or Vγ4$^-$Vγ7$^-$ GD3 cells (Extended Data Fig. 5c). There were no differences between DETC and GD3 cell viability and proliferation following their stimulation *in vitro* (Extended Data Fig. 5d). GD3 cells produced more IL-3 than cutaneous αβ T cells, ILCs, or other remaining CD45$^+$ cells, indicating that they are the major source of IL-3 in naïve, steady-state skin (Extended Data Fig. 5e). *Il3* expression in naïve skin was specific to GD3 cells (Extended Data Fig. 6a–b). This was independent of papain, as GD3 cells only expressed *Il3* or produced IL-3 when stimulated with PMA/Ionomycin or αCD3/CD28 (Extended Data Fig. 6c–d).

Given the unique production of IL-3 by GD3 cells, we hypothesized that this was the factor that drives allergen-induced itch. While IL-3 was unable to elicit itch on its own (Figure 3b), IL-3 enhanced allergen-induced itch in WT mice when i.d. injected before diverse allergens (Figure 3c; Extended Data Fig. 7a) and rescued papain-induced itch in *Tcrd*$^{-/-}$ mice (Figure 3d). IL-3, however, had no effect on IL-31-induced itch (Extended Data Fig. 7b), demonstrating the specificity of IL-3 priming to allergen-induced itch. The i.d. injection of IL-17A, produced only by dermal γδ T cells, or CCL3, produced non-specifically by dermal γδ T and GD3 cells, before papain did not impact itch (Extended Data Fig. 7c). Although the involvement of IL-4 and IL-13 in chronic itch was previously reported in an atopic dermatitis mouse model[7], papain-induced itch was unaffected in *Il4ra*$^{-/-}$ mice (Extended Data Fig. 7d). Consistent with a necessary role for IL-3 in sensory neuronal responses to allergens, papain-induced itch depended on global *Il3* and specific *Il3* expression in γδ T cells (Figure 3e–f). Because GD3 cells are the only apparent γδ T cell source of IL-3, these data indicate that GD3-derived IL-3 is required for allergen activation of sensory neurons.

IL-3 primes PEP1 neurons to allergens

We postulated that sensory neurons respond directly to IL-3 via the IL-3-specific receptor component IL-3Rα (*Il3ra*) and the IL-3, IL-5, and GM-CSF common component CD131 (*Csf2rb*) heterodimer[31]. *Il3ra* and *Csf2rb* were detected in acutely dissected DRG from

mice or human subjects[32] (Supplementary Fig. 5). To determine whether *Il3ra* was enriched within specific sensory neuronal subsets, we performed RNA fluorescence in situ hybridization (ISH) of DRG sections and paired *Il3ra* detection with that for marker genes of sensory neuronal subsets previously identified by scRNAseq[33–36]. *Il3ra* was significantly enriched in PEP1 and virtually absent in NP3 sensory neurons (Figure 3g), explaining the lack of effect of IL-3 on IL-31-induced itch (Extended Data Fig. 7b). In mice lacking *Il3ra*, papain-induced itch was impaired (Figure 3h). To determine if sensory neurons directly respond to IL-3 to promote allergic itch, we deleted *Il3ra* in sensory neurons via *Scn10a*. IL-3 enhanced papain-induced itch in control *Scn10a*[cre/+] mice expressing only one functional copy of the sodium channel *Scn10a* (Figure 3i), but not when *Il3ra* was eliminated from these cells (Figure 3j).

In vitro calcium imaging revealed that 8% of DRG neurons responded to IL-3, 20% to papain or AITC (a TRPA1 ligand), and 50% to capsaicin (a TRPV1 ligand) (Extended Data Fig. 7e–g). IL-3-responsiveness overlapped with papain- and capsaicin-responsive neurons but not with AITC-responsive neurons (Extended Data Fig. 7h). In the absence of TRPV1^{+} neurons, GD3 cells decreased, suggesting that there is bidirectional communication between these cells (Extended Data Fig. 7i). IL-3 pretreatment of DRG neurons *in vitro* increased the percentage of papain-responsive neurons (Figure 3k). We replicated these findings *in vivo*, assessing the effect of IL-3 on papain-induced calcium responses in trigeminal ganglia sensory neurons in live mice. Consistent with the *in vitro* results, we observed a significant increase in papain-induced sensory neuronal calcium activity among mice that underwent IL-3 pre-treatment, in contrast to mice pre-treated with sham DPBS (Figure 3l–m). Given the enrichment of *Il3ra* in PEP1 sensory neurons, we leveraged their expression of *Tac1*[33–36] to assess their role in allergic itch. Chemogenetic activation of *Tac1*-expressing cells caused mixed itch and pain responses (Extended Data Fig. 7j), while chemogenetic inhibition prevented papain, but not IL-31, induced itch (Extended Data Fig. 7k). These data indicate that IL-3 primes the allergen responsiveness of *Il3ra*-expressing PEP1 neurons.

IL-3 drives allergic immune initiation

The initiation of the allergic immune response, characterized by the migration of Th2-skewing CD301b^{+} dendritic cells (DCs) from the skin to the draining lymph node (dLN) followed by Th2 differentiation, depends on the release of substance P from allergen-activated sensory neurons[1,12]. Given the requirement for γδ T cells in allergen activation of sensory neurons, we hypothesized that the downstream allergic immune response would be defective in mice deficient in the GD3-IL-3 axis (Extended Data Fig. 8a). We tracked the migration of Kaede[red] Th2-skewing CD301b^{+} DCs from the skin to the dLN (Extended Data Fig. 8b) and found that papain immunization induced the migration of Th2-skewing CD301b^{+} DCs in WT Kaede, but not *Tcrd*^{−/−} Kaede mice (Figure 4a; Extended Data Fig. 8c–d). This finding was recapitulated in mice where *Il3* or *Il3ra* were deleted from *Tcrd*- or *Scn10a*-expressing cells, respectively; in these models, migratory antigen-bearing and activated Th2-skewing CD301b^{+} DCs were reduced in the absence of *Il3* in γδ T cells or *Il3ra* in sensory neurons (Figure 4b; Extended Data Fig. 8e–f). While papain elicits itch, acute scratching was not required for Th2-skewing CD301b^{+} DC migration to the dLN (Extended Data Fig. 8g).

Consistent with our finding of defective DC migration, the differentiation of IL-4^{+} and IL-4^{+}IL-13^{+} Th2 cells in the dLN was impaired in the absence of γδ T cells, *Il3*, *Il3ra*, or when *Il3* or *Il3ra* were deleted from *Tcrd-* or *Scn10a*-expressing cells, respectively (Figure 4c; Extended Data Fig. 9a–e). Defective Th2 differentiation in *Tcrd*^{−/−} mice resulted in no tissue swelling upon secondary challenge in a delayed-type hypersensitivity model (Extended Data Fig. 9f). These data indicate that the GD3-IL-3-sensory neuron signaling axis is required to initiate the allergic immune response.

IL-3 canonically signals through the JAK2-STAT5 cascade, wherein the phosphorylation of JAK2 leads to the phosphorylation of STAT5, a transcription factor that enters the nucleus, binding to DNA to promote the transcription of target genes[31]. We interrogated the mechanistic role of JAK2-STAT5 in promoting allergic itch and the initiation of the allergic immune response. In DRG neurons, IL-3 induced the phosphorylation of STAT5 that was prevented by the JAK2 phosphorylation inhibitor fedratinib (Figure 4d; Extended Data Fig. 10a). We previously established that sensory neuronal release of substance P was required for the initiation of the allergic immune response as measured by CD301b^{+} DC migration to the lymph node and Th2 differentiation[1]. Since IL-3 and its receptor were also required for CD301b^{+} DC migration and Th2 differentiation, we hypothesized that IL-3 induced substance P production through JAK2-STAT5. IL-3 enhanced STAT5 association with the promoter of the substance P gene *Tac1* beyond unprimed levels, while fedratinib (blocking upstream JAK2 phosphorylation) and STAT5-IN-1 (inhibitor of STAT5 DNA binding) impaired STAT5 binding (Figure 4e). Accordingly, in the absence of *Il3ra*, *Tac1* transcription was impaired in *Trpv1*^{+}, but not *Trpv1*^{-}. sensory neurons (Figure 4f). These transcriptional observations in *Tac1* corresponded to differential allergen-induced substance P release. In a JAK2- and STAT5-dependent manner, we found that IL-3 primed DRG neurons released significantly more substance P upon low-dose papain stimulation than unprimed neurons (Figure 4g). Thus, we established that JAK2-STAT5 regulates the transcription of *Tac1* and the amount of substance P released upon allergen stimulation.

With respect to the two outputs dictated by sensory neuronal IL-3 signaling, the phosphorylation of JAK2 was required for allergic itch and allergen-induced CD301b^{+} DC migration and Th2 differentiation (Figure 4h–j; Extended Data Fig. 10b–d). JAK1 was not required for allergic itch, nor did the inhibition of JAK2 impair histaminergic itch (Extended Data Fig. 10b). Consistent with its requirement in *Tac1* transcription and allergen-induced substance P release, STAT5 was disposable for acute allergic itch (Figure 4h) but required for allergen-induced, neuronally-dependent CD301b^{+} DC migration. Indeed, supernatant from IL-3 primed DRG neurons stimulated with papain induced the migration of CD301b^{+} DCs (Figure 4k). IL-3 priming of CD301b^{+} DC migration was dependent on both STAT5 (Figure 4k) and the presence of DRG neurons in the culture, as supernatant from cell-free wells treated with papain did not induce appreciable CD301b^{+} DC migration (Extended Data Fig. 10e). These data suggest that JAK2 and STAT5 exert distinct effects on the neuroimmune response to allergens: sensory neuronal JAK2 promotes allergic itch, while STAT5 governs the initiation of the allergic immune response.

Here we describe a γδ T cell-IL-3 pathway central to the allergen responsiveness of sensory neurons (Extended Data Fig. 10f). Previous studies found that sensory neurons

direct the initial immune response to allergens[1] and that chronic allergic inflammation of the skin elicits sensory neuronal activation[3–7]. Sitting upstream of this bi-directional neuroimmune circuit, we now propose that during naïve homeostatic conditions, GD3 cells and IL-3 determine the allergen activation "set-point" in sensory neurons through JAK2-STAT5 signaling to control sensory responses and neuropeptide transcription. Once an initial allergen exposure overcomes this threshold and chronic allergic inflammation is established, αβ T cells enter the skin and may further sensory neuronal responses through IL-3, IL-4, and/or IL-13[7,15]. However, the expression patterns of the relevant receptors (*Il3ra* in PEP1 neurons and *Il4ra* more broadly expressed[7,33,35]) explain why IL-3 promotes the activity of protease allergens that preferentially target PEP1 neurons[1,2,33,35], while IL-4 and IL-13 promote the responsiveness of chemical pruritogens, including histamine and chloroquine[7,33,35]. Given that a subset of atopic dermatitis patients fail dupilumab (anti-IL-4Rα monoclonal) therapy but respond to JAK inhibitors, this suggests that pathways alternative to IL-4Rα and JAK1[37], such as IL-3Rα and JAK2, are novel targets in atopic dermatitis and other itch disorders[38].

In addition to these findings, we characterized the physiological role of a rare epidermal γδ T cell lineage in mice. Similar to *Skint1*^{−/−} FVB/N-Tac mice, hominoids, including humans, harbor a *SKINT1*-like gene that is inactivated by multiple mutations, rendering these primates devoid of a direct analog to mouse Vγ5[+] DETCs[28]. Nonetheless, humans contain a population of epidermal γδ T cells with a poorly understood etiology and function[29,39]. Comparing mouse GD3 cells to healthy human skin cells revealed that GD3 cells are transcriptionally similar to human γδ T cells. Thus, our data suggest that GD3 cells may be the relevant mouse counterpart to human epidermal γδ T cells. Whether GD3 cells have other physiological roles or if their production of IL-3 impacts other cells expressing IL-3Rα has not yet been established in homeostatic or pathophysiologic situations. The allergic immune response may have evolved to protect the host from environmental toxins, offering a potential beneficial role of GD3 cells for the organism[40]. Given that the number of GD3 cells is highly receptive to environmental cues, we propose that this pathway could explain individual differences in allergic susceptibility. Those questions notwithstanding, our study suggests that correcting an overabundance of GD3 cells, their production of IL-3, sensory neuronal IL-3Rα, or sensory neuronal JAK2-STAT5, would improve the outcome of patients with allergic disease and prevent allergen sensitization.

Materials and Methods

Mice

Experiments involving animals were approved by the Massachusetts General Hospital or Harvard Medical School Institutional Animal Care and Use Committee (IACUC). Mice were maintained and bred in a specific-pathogen-free (SPF) facility in ventilated cages, a maximum of 5 mice per cage, on a 12-hour day-night cycle, at 20–25°C and 35–65% humidity, and provided food and water ad libitum. Experimental mice were 5–16 weeks of age unless otherwise noted. Male and female mice were used in all experiments unless specifically noted, and comparisons were made between age and sex-matched controls. Power calculations were conducted to determine sample sizes. Mice were placed into

groups depending on their genotype; when possible, mice were ranomdized. Behaviorial experiments were blinded, while immunologic experiments were not.

Wild-type C57BL/6 (WT; 556) mice were purchased from Charles River Laboratories (Wilmington, MA). C57BL/6 WT (000664), $Tcrd^{-/-}$ (B6.129P2-$Tcrd^{tm1Mom}$/J; 002120), $Rag2^{-/-}$ (B6.Cg-$Rag2^{tm1.1Cgn}$/J; 008449), $Tcra^{-/-}$ (B6.129S2-$Tcra^{tm1Mom}$/J; 002116), $muMT^{-/-}$ (B6.129S2-$Ighm^{tm1Cgn}$/J; 002288), $Skint1^{+/+}$ FVB/NJ (001800), $Tcrd^{CreER}$ (B6.129S-$Tcrd^{tm1.1(cre/ERT2)Zhu}$/J; 031679), ROSA-DTA (B6.129P2-$Gt(ROSA)26Sor^{tm1(DTA)Lky}$/J; 009669), $Scn10a^{cre}$ (B6.129(Cg)-$Scn10a^{tm2(cre)Jwo}$/TjpJ; 036564), $Ai9$ (B6.Cg-$Gt(ROSA)26Sor^{tm9(CAG-tdTomato)Hze}$/J; 007909), $Ai95D$ (B6J.Cg-$Gt(ROSA)26Sor^{tm95.1(CAG-GCaMP6f)Hze}$/MwarJ; 028865), $Vglut2^{cre}$ (B6J.129S6(FVB)-$Slc17a6^{tm2(cre)Lowl}$/MwarJ; 028863), $Tac1^{cre}$ (B6;129S-$Tac1^{tm1.1(cre)Hze}$/J; 021877), $GqDREADD$ (B6N;129-Tg(CAG-CHRM3*,-mCitrine)1Ute/J; 026220), and $GiDREADD$ (B6.129-$Gt(ROSA)26Sor^{tm1(CAG-CHRM4*,-mCitrine)Ute}$/J; 026219) mice were purchased from The Jackson Laboratory (Bar Harbor, ME). $Skint1^{-/-}$ FVB/NTac mice were purchased from Taconic Biosciences (Germantown, NY). $Cpa3^{cre}$ mice were originally from Hans-Reimer Rodewald (German Cancer Research Center). $Tcrd^{GDL}$ mice were originally from Immo Prinz (Medizinische Hochschule Hannover). Germ-free (GF) mice were acquired from the Massachusetts Host-Microbiome Center. Skin samples from pet shop mice were kindly provided by David Masopust (University of Minnesota). $Il3^{-/-}$, $Il3ra^{-/-}$, $Il3^{GFPfl/fl}$, and $Il3ra^{fl/fl}$ mice were generated and provided by Cameron McAlpine, Ben Kleinstiver, and Filip Swirski at Massachusetts General Hospital[41,42]. $Trgv4^{-/-}$ mice were originally from Daniel Mucida (Rockefeller). $Il4ra^{-/-}$ mice were originally from Fred Finkelman (University of Cincinnati). $Trpv1^{DTR}$ mice were originally from Mark Hoon (NIH). Kaede mice were originally from Osami Kanagawa (Riken). $Tcrd^{CreER}$ (referred to as $iTcrd^{cre}$) were crossed to ROSA-DTA or $Il3^{GFPfl/fl}$ to generate tamoxifen-inducible $iTcrd^{DTA}$ or $iTcrd^{cre/+}Il3^{GFPfl/fl}$ mice, respectively. $Scn10a^{cre}$ were crossed to $Ai9$ or $Il3ra^{fl/fl}$ to generate $Scn10a^{tdTomato}$ or $Scn10a^{cre/+}Il3ra^{fl/fl}$ mice, respectively. $Vglut2^{cre}$ was crossed to $Ai95D$ to generate mice for $in\ vivo$ calcium imaging. $Tac1^{cre}$ were crossed to $GqDREADD$ or $GiDREADD$ to generate $Tac1^{cre/+}GqDREADD$ or $Tac1^{cre/+}GiDREADD$ mice, respectively. Kaede was crossed to $Tcrd^{-/-}$ to generate Kaede x $Tcrd^{-/-}$ mice.

To control for differences in commensal microbes among colonies, all experiments utilizing $Cpa3^{cre/+}$, $Tcrd^{GDL}$, $iTcrd^{cre/+}$, $Scn10a^{cre/+}$, and $Tac1^{cre/+}GqDREADD$ mice were performed with littermate controls bred in our facility. All other experiments comparing WT to experimental mouse lines were performed with colony control WT mice originally from The Jackson Laboratory, but bred in our facility, except in Figure 1b, Extended Data Figure 1d (chloroquine), Extended Data Figure 1e, and Extended Data Figure 8i, which used controls purchased from Charles River Laboratories. In experiments that only used WT mice, the mice were purchased from Charles River Laboratories and utilized immediately upon arrival in our laboratory. FVB/N mice came from different colonies to enable $Skint1$ studies ($Skint1^{+/+}$, Jax; $Skint1^{-/-}$, Taconic). In supernatant transfer models, donor cells were the same strain and colony of origin as the recipient mice.

Experimental mouse models

Immunizations

Under brief isoflurane anesthesia, mice were intradermally (i.d.) immunized with 25 μL in the cheek (behavior), top of the foot (DC migration and T cell differentiation), or pinnae (immune cell harvest and delayed-type hypersensitivity). Immunizations included papain [50 μg previously frozen, 1 μg freshly prepared (Millipore Sigma), or 5 μg freshly prepared (Creative Enzymes), to normalize for differences in enzymatic activity]; 100 or 20 μg (low-dose) house dust mite (HDM) and 100 or 10 μg (low-dose) *Alternaria alternata* (Greer Laboratories); 2,500 or 500 PNU (low-dose) fire ant (ALK); 5 mosquitoes worth of mosquito saliva; 50 μg histamine, chloroquine, and ovalbumin (ova; Millipore Sigma); 20 μg capsaicin (Cayman Chemical); 2.5 μg IL-31 (Peprotech); 1.25 μg clozapine-N-oxide (CNO; Millipore Sigma); culture supernatant as indicated. Mosquito saliva was generated as previously described[43] from adult *Aedes aegypti* females (Liverpool strain). Soluble substances were dissolved in DPBS (Corning), while insoluble substances were dissolved in corn oil or DMSO (Millipore Sigma). For chronic papain injections, mice were i.d. injected with 5 μg papain in 25 μL DPBS in the pinnae on days 0, 2, 4, 7, 9, and 11. Mice were euthanized on day 14, and pinnae were harvested and processed following the *Isolation of immune cells from mouse dermis and epidermis* protocol.

Behavior

Mice were moved from the animal facility to a private room in our laboratory and separated into individual cages where they habituated for 2 hours. Following i.d. cheek injection with 25 μL of indicated stimuli, a video was recorded from above, and scratching at the injection site (with the hind paw) was tabulated. A 20-minute video was recorded for chloroquine, HDM, capsaicin, and *Alternaria* in WT vs. $Tcrd^{-/-}$ mice (Figure 1b and Extended Data Figure 1d–e) and papain in WT vs. $Il4ra^{-/-}$ mice (Extended Data Fig. 8i). A 60-minute video was recorded for mosquito saliva experiments. In all other behavior experiments, a 30-minute video was recorded. In spontaneous nonspecific itch experiments (Figure S1b), no injection was performed, and scratch at any skin site (cheek, pinnae, flank, side, back, etc) was quantified over 30 minutes.

Depletion of γδ T cells in Tcrd^GDL mice

Tcrd^GDL mice express the human diphtheria toxin receptor (DTR) in *Tcrd*-expressing cells[44]. *Tcrd^WT* and *Tcrd^GDL* mice were injected intraperitoneally (i.p.) with 0.5 μg of diphtheria toxin (DT; Millipore Sigma) every other day for 2 total injections, then rested for 3 days. Behavior and flow cytometry were performed after the rest period.

Tamoxifen-induced cre in iTcrd^cre mice

We crossed *iTcrd^cre* with *ROSA-DTA* mice to generate tamoxifen-inducible diphtheria toxin A in *Tcrd*-expressing cells[45,46]. *iTcrd^control* and *iTcrd^DTA* or *iTcrd^cre/+Il3^{+/+}* and *iTcrd^cre/+Il3^{fl/fl}* mice were injected i.d. with 0.5 mg of tamoxifen (Cayman Chemical) on two consecutive days, then rested for 4 days. Behavior, flow cytometry of the pinnae, dendritic cell migration, or T cell differentiation assays were performed after the rest period.

Epidermal DETCs and GD3 cells were preferentially depleted *iTcrd^DTA* mice, likely due to their high expression of *Tcrd*, as previously found[45].

Mouse model of dry skin

To induce dry skin, we modified the acetone:diethyl ether + water (AEW) model as previously described[47,48]. Pinnae was treated twice daily with AEW or sham for 4 days. A 1:1 ratio of actone:diethyl ether was applied to the skin using a soaked gauze for 15 seconds, then H_2O was applied to the same site for 30 seconds. Following a rest period, experiments were performed on day 8.

Depletion of Trpv1⁺ sensory neurons in Trpv1^DTR mice

Over a 14-day period, WT and *Trpv1^DTR* mice were injected i.p. with 0.2 μg of DT (Millipore Sigma) every day for 5 days, then rested for 2 days. After the final DT injection, mice rested for 7 days. Deletion of *Trpv1*-expressing sensory neurons was confirmed using the tail-flick assay[1]. Flow cytometry was performed after the rest period.

Supernatant transfer and cytokine instillation

Tissue-culture-treated U-bottom 96-well plates (Corning) were incubated with 50 μL of purified αCD3 (2 μg/mL, BioLegend) for 2 hours at 37°C, then washed 4 times with DPBS. Dermal γδ T cells, DETCs, and GD3 cells were FACS isolated and resuspended in fully-supplemented RPMI [RPMI (Corning) supplemented with 10% FBS, 1% Penicillin-Streptomycin, 1% Glutamax, 1% HEPES, 1% NEAA (Gibco), 1% sodium pyruvate (Gibco), and 0.1% 2-mercaptoethanol (Gibco)]. 1,000–4,000 cells/well were incubated at 37°C in 5% CO_2. In wells coated with αCD3, purified αCD28 (2 μg/mL) was added to the fully-supplemented RPMI. In one control experiment, wells were coated with αCD3, and purified αCD28 (2 μg/mL) was added to the fully-supplemented RPMI, but no cells were plated. After 5 days, cell-free supernatant was harvested, snap-frozen, and stored at −80°C.

Following 2 hours of habituation, as described in the *Behavior* protocol, mice were i.d. immunized with 25 μL cell-free supernatant derived from unstimulated or stimulated dermal γδ T cells, DETCs, or GD3 cells. 30 minutes later, mice were i.d. immunized with 1 or 5 μg papain. Videos were recorded following papain injection, and scratch bouts were tabulated. In the indicated experiments, DPBS or 5 μg recombinant mouse IL-3, IL-17A, or CCL3 (Peprotech) in DPBS was injected 30 minutes before papain, HDM, *Alternaria alternata*, fire ant, or IL-31. Videos were recorded in the 30 minutes following cytokine immunization (when indicated) or following the subsequent papain injection.

Co-housing germ-free mice

To re-introduce a commensal microbiota to germ-free (GF) mice, female C57BL/6 SPF mice from Charles River were co-housed along with female GF mice for 5 weeks in our colony. These mice became exSPF and exGF. Following co-housing, flow cytometry was performed.

Trigeminal ganglion in vivo *calcium imaging*

Vglut2^cre were crossed to *Ai95D* to allow for calcium imaging of trigeminal ganglia as described previously[49]. Briefly, mice were induced and maintained at surgical plane

anesthesia by intraperitoneal injection of ketamine (100mg/kg) and xylazine (10mg/kg), and a unilateral craniotomy and hemispherectomy performed to expose the surface of the trigeminal ganglion. Illumination was provided with a collimated 470nm light emitting diode through a 10x, 0.3 numerical aperture air objective. Images were acquired at 10Hz with 35ms exposure time using a CMOS camera. For each animal, we designated a single field of view guided by the criterion that it contained neurons displaying robust calcium responses upon the indentation of the cheek skin. In each experiment, before assessing the effect of IL-3, GCaMP activity was imaged in response to cheek indentation and 5 minutes of baseline activity. Subsequently, mice were i.d. injected with 5 μg (25 μL) IL-3 or sham DPBS (25 μL) at the location where mechanical indentation was performed. This was followed by three 5-minute imaging sessions, covering 0–5, 10–15, and 20–25 minutes post-injection. 30 minutes after IL-3 or DPBS priming, the mice received an i.d. challenge injection of 5 μg (25 μL) papain followed again by three 5-minute imaging sessions capturing 0–5, 10–15, and 20–25 minutes post-papain treatment.

Images of GCaMP fluorescence were normalized to a low-pass spatial filtered image of each frame to correct for fluorescence bleaching and non-focal plane-derived fluorescence transients, and motion corrected using a Python implementation of TurboReg[50]. Regions of interest containing active cells were identified by adaptive thresholding of heat maps constructed by measuring correlation of each pixel to neighboring pixels, with manual curation of region of interests defined automatically. Region of interest masks were refined by constrained non-negative matrix factorization[51], after which modified z-scored activity traces were extracted as mean fluorescence intensity normalized to median absolute deviation of each trace. Proportion of time above threshold (z-score above 3.5) was used as a metric of ongoing activity in each neuron during baseline measurement and after papain injection, with cells above threshold in at least 15% of time points over a 15 minute of imaging time classified as spontaneously active.

Chemogenetic manipulation of Tac1-expressing cells

Clozapine-n-oxide (CNO) is a pharmacologically inert ligand that binds to DREADDs, leading to the chemogenetic activation of *Tac1*-expressing cells in the "*GqDREADD*" mouse and inhibition in the "*GiDREADD*" mouse[52]. To elicit the chemogenetic activation of *Tac1*-expressing cells, *Tac1^{cre/+}GqDREADD* mice were i.d. immunized with 1.25 μg CNO in the cheek. A 90-minute video was recorded from above. Cheek wipes (with the fore paw) and cheek, flank, or pinnae scratch bouts (with the hind paw) were tabulated. To elicit the chemogenetic inhibition of *Tac1*-expressing cells, *Tac1^{cre/+}GiDREADD* mice were i.d. immunized with 1.25 μg CNO in the cheek 30 minutes before 5 μg papain or 2.5 μg IL-31 was injected at the same site. A 30-minute video was recorded from above, and scratching at the injection site was counted.

Dendritic cell migration

Kaede mice express a photoconvertible protein that switches from green to red upon exposure to violet light[53]. Following the exposure of Kaede skin to violet light, cell migration throughout the organism can be tracked by assessing cells that were photoconverted from Kaede^{green} to Kaede^{red}. The skin of Kaede mice was photoconverted

by exposing the dorsal aspect of the feet to light generated by a Bluewave LED visible light curing unit (Dymax) with a 420 nm bandpass filter (Andover Corp). The exposure lasted 5 minutes, and the light was positioned 7.5 cm away from the dorsal feet. Immediately after photoconversion, the dorsal foot was immunized with 25 μL as indicated. Internal controls were used in these experiments, as one dorsal foot received ova alone (control antigen) while the other received ova+papain. In some experiments, cell-free supernatant from DRG neuron cultures was injected into the dorsal foot as indicated (culture supernatant was prepared as described in the *Substance P release for dorsal root ganglia neurons* protocol). In all experiments, paired analyses were used to evaluate the migration of DCs to the draining lymph node (dLN). 24 hours after immunization, the popliteal LN was harvested and digested at 37°C in digestion buffer: RPMI supplemented with DNase I (100 μg/mL; Roche), Dispase II (800 μg/mL; Millipore Sigma), Collagenase P (200 μg/mL; Millipore Sigma), and 1% FBS. Every 7 minutes, the digestion buffer was removed and placed into RPMI supplemented with 2 mM EDTA and 1% FBS on ice. Fresh digestion buffer was added to the LNs. Tubes were vigorously shaken before and after each addition of fresh digestion buffer. This process was repeated until no fragment of LN tissue remained. Single-cell suspensions were filtered through a 70 μm cell strainer before flow cytometry was performed.

To track the migration of DCs in other mouse strains that lack photoconvertible skin cells, 5 μg fluorescently labeled ova-AF647 (Fisher Scientific) was i.d. injected with 45 μg ova and 50 μg papain in the dorsal aspect of the feet. One foot received ova, while the other received ova+papain. 24 hours after immunization, the popliteal LNs were harvested and processed as above. In migratory (CD11c^{+}IAIE^{high}) CD301b^{+} DCs, ova-AF647^{+}PDL2^{+} cells marked activated and antigen-bearing Th2-skewing DCs.

In some experiments, DC migration was assessed in mice anesthetized with isoflurane (<30 seconds of sedation) or ketamine/xylazine (>30 minutes of sedation). With ketamine/xylazine, mice remain sedated throughout the itch response to primary allergen immunization, largely completed within 20 minutes after injection[1]. In *Scn10a[cre/+]* experiments, only male mice were used.

T cell differentiation

Mouse footpads were immunized with 25 μL as indicated. Internal controls were used in these experiments, as one dorsal foot received ova alone (control antigen) while the other received ova+papain. 5 days following immunization, the dLN was harvested and dissociated in DPBS using the coarse end of a SuperFrost Plus Microscope Slide and the base of a curved forcep. Single-cell suspensions were filtered through a 70 μm cell strainer. 2×10^6 LN cells were added to a 1.5 mL Eppendorf tube (Fisher Scientific) and resuspended in 1 mL fully-supplemented RPMI with PMA (50 ng/mL; Millipore Sigma), Ionomycin (1 μg/mL; Millipore Sigma), and Protein Transport Inhibitor (1:1000, BD Biosciences). Samples were incubated for 3 hours at 37°C in 5% CO_2. Samples were washed twice with FACS Buffer; then, cells were incubated in FACS Buffer containing fluorescent-conjugated antibodies targeting surface antigens for 15 minutes at 4°C. Following fixation with 4% PFA for 8 minutes at room temperature, fluorescent-conjugated antibodies targeting intracellular

cytokines were added to each sample in 1x eBioscience™ Permeabilization Buffer for 1 hour at 4°C. Cells were washed twice with DPBS, then assessed by flow cytometry.

Delayed-type hypersensitivity

WT and $Tcrd^{-/-}$ mice were i.d. injected in bilateral cheeks with 25 μL of 50 μg ova and 50 μg papain on days 0 and 2. On day 12, one pinna was injected with 25 μL of 50 μg ova. Pinnae thickness was measured on day 12 before the injection, and 24 (day 13) and 48 (day 14) hours later.

Inhibitor treatment

Mice were i.p. injected with 100 μL of 10 mg/kg fedratinib (targeting JAK2; Selleck Chemicals), 10 mg/kg upadacitinib (targeting JAK1; Selleck Chemicals), or 10 mg/kg STAT5-IN-1 (targeting STAT5; Millipore Sigma) dissolved in corn oil containing 10% DMSO (Millipore Sigma). Behavior to papain or histamine was evaluated 2 hours later in WT mice treated with or without the inhibitors. 2 hours after fedratinib injection, the dorsal feet of Kaede mice were photoconverted and immunized with ova or ova+papain. The dLN was harvested 24 hours later to assess the migration of DCs. 2 hours after fedratinib injection, the dorsal feet of WT mice were immunized with ova or ova+papain. 5 days later, T cell differentiation was assessed in the popliteal dLN.

Isolation of immune cells from mouse dermis and epidermis

To isolate cutaneous cells from the skin, pinnae were removed from euthanized mice and weighed. Forceps were used to pull apart the dorsal and ventral sides of the pinnae. Once separated, the epidermis was attached to a piece of Flexigrid™ tape. In some experiments, to isolate cutaneous cells from the cheek and dorsal foot, mice were anesthetized with ketamine/xylazine, and hair was removed from the cheek or dorsal foot skin using Veet. 24 hours later, the cheek and dorsal foot skin were harvested from euthanized mice and weighed. The epidermis was then attached to a piece of Flexigrid™ tape. With the dermis-side down, the skin was floated on Dispase II (3 mg/mL, Millipore Sigma) in DMEM (Corning) for 90–120 minutes at 37°C in 5% CO_2. The dermis was removed from the epidermis and vigorously minced before digestion in 5 mL Eppendorf tubes (Fisher Scientific) containing Liberase™ (25 μg/mL, Millipore Sigma), DNAse I (75 μg/mL, Millipore Sigma), and 10 μM HEPES (Corning) in DMEM. The epidermis was digested in 5 mL Eppendorf tubes containing Collagenase IV (2 mg/mL, Millipore Sigma) in DPBS. 5 mL Samples were placed at 37°C in 5% CO_2 for 45 minutes and vigorously shaken every 9 minutes. Tubes were immediately placed on ice, and 500 μL heat-inactivated FBS (Millipore Sigma) and 15 μL 0.5 M EDTA (Invitrogen) were added. Dermal fragments were repeatedly aspirated and flushed through an 18-gauge needle. Finally, dermal and epidermal suspensions were twice filtered through a 70 μm cell strainer (Corning or Biologix) before downstream use.

Isolation of cells from mouse dorsal root ganglia

Dorsal root ganglia (DRG) were carefully dissected from mice and placed into a 15 mL Falcon® tube (Corning) containing DMEM supplemented with 10% FBS and 1% Penicillin-Streptomycin (Millipore Sigma). DRGs were centrifuged at 1,000 rpm for 5 minutes, then digested for 70 minutes in 3 mL of Collagenase A (1.25 mg/mL, Millipore Sigma) and Dispase II (2.5 mg/mL, Millipore Sigma) on a 37°C shaker set to 150 rpm. 10 mL of DMEM supplemented with 10% FBS and 1% Penicillin-Streptomycin was added, then the dissociated DRGs were washed twice in DPBS supplemented with 1% Penicillin-Streptomycin and 1% GlutaMax (Gibco) before being resuspended in 1 mL Neurobasal media A (NBM; Thermo Fisher Scientific) supplemented with 1x B-27 (Thermo Fisher Scientific) and 1% Penicillin-Streptomycin. DRGs were gently pipetted for 5–10 minutes using a P1000 pipette tip. This process was repeated using a P200 pipette tip. DRGs were layered on top of a 28% and 12.5% gradient of Percoll (VWR) diluted in supplemented NBM. The DRG cell suspension was centrifuged at 1,300g for 10 minutes at room temperature with no acceleration or brake. The cell pellet was then resuspended in supplemented NBM and filtered through a 70 μm cell strainer before downstream use.

DPBS. To isolate immune cells from DRGs, the Percoll gradient was not performed.

Flow cytometry and cell sorting

Single-cell suspensions were incubated at 4°C for 15 minutes in FACS Buffer (0.5% FBS in DPBS) containing fluorescent-conjugated antibodies. Dead cells were excluded using Fixable Viability Dye eFluor 780 (eBioscience) added to antibody (Ab) preparations at a dilution of 1:2000. TruStain fcX™ (anti-mouse CD16/32; BioLegend) was added to Ab preparations at a dilution of 1:200. Ab-tagged cells were washed twice with DPBS. If necessary, single-cell suspensions were fixed in 4% Paraformaldehyde (PFA; Electron Microscopy Sciences) for 8 minutes at room temperature and washed twice with DPBS. Due to the autofluorescence of dermal macrophages, the lineage markers CD68, CD11b, and CD11c were used in the indicated skin analyses to exclude them. Purified anti-mouse TCR Vγ7 (BioLegend) was conjugated to AF647 using a Lightning-Link Alexa Fluor 647 Conjugation kit (Abcam). Ab-tagged cells were analyzed on a CytoFLEX S flow cytometer (Beckman Coulter) or a Cytek Aurora (Cytek Biosciences) or sorted on a MA900 multi-application cell sorter (SONY, Cell Sorter Software v3.3.2). Flow cytometric data were acquired using CytExpert v2.3 (Beckman Coulter) or SpectroFlo v3.2.1 (Cytek Biosciences) software, and fcs files were analyzed using FlowJo version 10 (TreeStar). The Abs used in this study are listed in Supplementary Table 3.

The following gating strategies were used: Dermal γδ T cells were live Lineage⁻CD3⁺TCRγδ^intermediate. Dendritic epidermal T cells (DETCs) were live Lineage⁻CD3⁺TCRγδ^high Vγ5⁺. Epidermal GD3 cells were live Lineage⁻CD3⁺TCRγδ^high Vγ5⁻. In Extended Data Figure 2b, γδ T cells were live CD45⁺Lineage⁻CD3⁺TCRγδ⁺. In Extended Data Figure 2f, αβ T cells were live Lineage⁻CD3⁺TCRβ⁺. Lineage markers: CD68, CD11b, CD11c. In Extended Data Figure 9e, GD3 cells were live CD45⁺Lineage1⁻CD3⁺TCRγδ^high Vγ5⁻, αβ T cells were

live CD45$^+$Lineage1$^-$CD3$^+$TCRβ$^+$, helper-like innate lymphoid cells (ILCs) were live CD45$^+$Lineage1$^-$Lineage2$^-$CD3$^-$Thy1.2$^+$, and other were all remaining CD45$^+$ cells. Lineage1 was CD68, CD11b, and CD11c. Lineage2 was NK1.1, B220, and CD19. Th2-skewing dendritic cells (DCs) were live CD11c$^+$IAIE^{high}CD301b$^+$. The migration of Th2-skewing dendritic cells to the draining lymph node was assessed by Kaede^{red} positivity, while activation and antigen uptake were monitored by PDL2 and ova-AF647 positivity, respectively. IL-4$^+$ Th2 cells were live CD4$^+$CD44^{high}IL-4$^+$. IL-4$^+$IL-13$^+$ Th2 cells were live CD4$^+$CD44^{high}IL-4$^+$IL-13$^+$.

Single-cell RNA and TCR sequencing: mouse

A single-cell suspension of skin cells was generated from 30 pooled WT mice. Dermal γδ T cells, DETCs, and GD3 cells were FACS sorted into 50% fully-supplemented RPMI and 50% FBS. After washing the sorted cells with FACS Buffer, each population was loaded as a separate channel on the Chromium 10x Genomic v1.1 platform (10X Genomics). Libraries were prepared using the Chromium Single Cell 5' Library Construction Kit. Gene expression (GEX) and TCRγδ (TCR) libraries were generated from the cDNA produced through the Chromium chemistry. For the TCR libraries, custom primers were used to amplify TCRγδ chains following a protocol that was previously described[54]. Nucleic acid products were separated using SPRIselect beads (Beckman Coulter). Libraries were quantified using the Bioanalyer High Sensitivity DNA analysis kit (Agilent). Sequencing of GEX libraries was performed using the Nextseq 500/550 High Output kit v2.5 (75 cycles; Illumina), while TCR libraries were sequenced with the Nextseq 500/550 High Output kit v2.5 (150 cycles; Illumina). Sequencing was performed on the NextSeq 550 (Illumina).

Read alignment and quantification

Raw sequencing data was pre-processed with CellRanger (v6.1.2, 10X Genomics) to demultiplex FASTQ reads, align reads to the mouse reference genome (mm10, v2020-A from 10x Genomics), and count unique molecular identifiers (UMI) to produce a cell x gene count matrix[55]. All count matrices were then aggregated with Pegasus (v1.6.0, Python) using the *aggregate_matrices* function[56]. Droplets with >20% mitochondrial UMI or <500 unique genes detected were deemed low-quality cells or empty droplets and were filtered out of the matrix prior to proceeding with downstream analyses. The counts for each remaining cell in the matrix were then log-normalized by computing the log1p(counts per 100,000). Following the application of quality control filters on the data, 28,765 high-quality cutaneous γδ T cells were recovered (Supplementary Table 1).

Single-cell RNAseq analysis

For clustering, 2,000 highly variable genes were selected using the *highly_variable_features* function in Pegasus and used as input for principal component analysis. The resulting principal components were used as input for Uniform Manifold Approximation and Projection (UMAP) algorithm (spread=1, min-dist=0.5). The number of principal components used for each clustering (global = 35 ; GD3 = 26 ; DETC = 20) was decided via Molecular cross-validation (MCV)[57]. In this MCV approach, the raw counts for each cell were randomly split to obtain two count matrices, A and B, whose sum was equal to

the original count matrix. The top K principal components and loadings of the centered and scaled matrix A' were then used to reconstruct matrix B' and estimate an MCV loss with the mean squared error. The MCV losses for the top K principal components between 2 and 100 were estimated and the K that minimized MCV loss was used in downstream analyses. Comparisons between the different cell types were performed using the *de_analysis* function from Pegasus. log2FC values were visualized with ggplot2 (R 3.3.3).

Single-cell TCRseq analysis

Raw sequencing data was pre-processed with CellRanger (v7.0.0, 10X Genomics) to demultiplex FASTQ reads and align reads to the mouse immune repertoire genome (GRCm38, v7.0.0 from 10x Genomics). Resulting TCRs were filtered to those that were productive (i.e. no stop codons), had at least two UMIs, and aligned with the single-cell data. For cells with multiple captured rearranged TCR chains, the one with the greatest number of UMIs was used for downstream analysis.

Estimation of RNA velocity

Count matrices of spliced and unspliced transcript abundances were calculated using velocyto (v0.17.15, Python)[58]. These matrices underwent dimensionality-reduction via principal component analysis (PCA) as described above and were used to compute a k-nearest neighbor graph (k=30) that was used as input to estimate cellular velocity with scVelo (v0.2.4, Python)[59]. CellRank (v1.5.1, Python) was used to estimate initial and terminal states and these estimations were used to recover latent time with the *recover_latent_time* function with scVelo[60]. Velocity streamlines were plotted on UMAP embeddings with the *velocity_embedding_stream* function and the lineage driver genes associated with the inferred trajectory were calculated with the *lineage_drivers* function from CellRank. The top 100 genes driving the RNA velocity of the GD3 lineage are presented in Supplementary Table 2.

Single-cell RNA sequencing: human

Two independent public datasets of human skin were re-analyzed[29,30] to compare the relationship between mouse GD3 cells and human skin cells.

Datasets used and reviews of their cohorts

The raw gene count matrix from Gellatly et al.[29] was obtained from https://vitiligo.dolphinnext.com/index.html. Cells derived from this study were collected through suction blistering of the skin and sequenced using a modified inDrop protocol. This method enriches epidermal cells, which was of particular interest given that GD3 cells are found in the mouse epidermis. The public dataset was filtered to include only 'normal' healthy controls, i.e., those with no auto-immune or inflammatory skin diseases. This dataset included seven individuals, consisting of four women and three men aged 11 to 57.

Raw gene count matrices from Reynolds et al.[30] were obtained from https://zenodo.org/record/4569496. Skin cells from this study were obtained from mammoplasty surgery surplus and sequenced following 10x protocol. As genes in the 'normal' healthy

dataset (healthy.h5ad) were already filtered, raw counts from the full dataset (submission_210120.h5ad) were obtained by matching droplets by barcode. The final dataset included five healthy female individuals aged 25 to 60.

Pre-processing and clustering

Gene count matrices from both human datasets were re-processed similarly to the processing of the mouse data. The Reynold's dataset was first filtered to include only cells previously annotated as T and NK cells; all lineages in the Gellatly dataset were kept due to the smaller dataset size. Higher-quality droplets were then selected based on the number of unique genes and percent of mitochondrial UMIs (>250 genes, <20% mitochondrial UMIs in the Reynolds dataset; >250 genes in the Gellatly dataset (no mitochondrial UMIs provided)). Similarly to the mouse dataset, counts were log-normalized by computing the log1p(counts per 100,000).

To cluster cells in each dataset, 2,000 highly variable genes were selected using the highly variable features function of Pegasus. These genes were then used in molecular cross-validation to obtain the number of principal components (PCs) for down-stream analyses (20 PCs Gellatly, 40 PCs Reynolds). To account for variability between donors and sequencing time, the resulting PC scores were batch-corrected by sample using harmony-pytorch v0.1.4. The harmonized PCs were used as input for Leiden clustering and creating a uniform manifold approximation and projection (UMAP).

Gene set scoring

DE analysis was run between the GD3 and dermal $\gamma\delta$ T cell types of the mouse dataset using Pegasus's de_analysis function, and genes were ranked by t-statistic to obtain a list of the top 25 distinguishing genes between cell types. The Vγ5$^+$ DETC cell type was excluded as it is not observed in humans due to the inactivation of the *SKINT1*-like gene, which its equivalent is required for Vγ5$^+$ DETC development in mice[28]. Mouse genes were then converted to their human homologs to be used as reference gene sets in Gene Set Enrichment Analysis (GSEA) using Ensembl's biomaRt release 108. Cells in the human datasets were pseudobulked by sample, and DE analysis was run using limma v3.54.2 to compare one cluster against all other clusters to obtain genes distinguishing the individual clusters. The R package fgsea v1.24.0 was then used to run GSEA on each human cluster, where the distinguishing genes ranked by t-statistic were provided as input to investigate trends relating to the GD3 gene set used as a reference.

One limitation of the previous approach is that clustering resolution may affect what signal is picked up in the lists of distinguishing genes. To identify potential signals on a smaller scale, average z-scores of gene expression were computed for each cell using the GD3 gene set. These averaged z-scores were then plotted in UMAP space to find areas of high expression.

Confocal immunofluorescence of epidermal sheets and intact skin

Pinnae were removed from euthanized mice, and forceps were used to pull apart the dorsal and ventral sides of the pinnae. The epidermis was attached to a piece of Flexigrid™ tape. Pinnae were floated on pre-warmed 0.47 M Ammonium thiocyanate (Millipore Sigma) in

DPBS for 15 minutes at 37°C in 5% CO_2, with the dermal side facing down. The dermis was carefully peeled away from the epidermis. Pieces of tape with epidermis attached to them were rinsed twice in DPBS. Epidermal sheets were fixed by floating them on 4% PFA for 8 minutes at room temperature. Epidermal sheets were fixed with gentle shaking on a plate shaker. Samples were washed 3 times in 2% heat-inactivated goat serum (Jackson ImmunoResearch) and 0.2% Triton X-100 (Millipore Sigma) in DPBS for 10 minutes during each wash cycle, then incubated for 2 hours at room temperature in 500 μL of 10% heat-inactivated goat serum and 0.2% Triton X-100 in DPBS containing fluorescent-conjugated antibodies of interest. Confocal immunofluorescence of epidermal sheets utilized the following antibodies: 1:50 anti-TCRγδ (BV421; clone GL3; 118120; BioLegend), 1:50 Vδ4 (eFluor 600; clone GL2; 50–5702-80; eBioscience), and 1:200 Vγ5 (PE; clone 536; 137504; BioLegend). Samples were washed 3 times in 2% heat-inactivated goat serum and 0.2% Triton X-100 in DPBS for 10 minutes during each wash cycle. Epidermal sheets were mounted onto SuperFrost Plus Microscope Slides (Fisher Scientific) with one drop of ProLong™ Diamond Antifade Mountant (Invitrogen). In experiments utilizing intact pinnae, wherein the dermis was not separated from the epidermis, pinnae from *Scn10a^{tdTomato}* mice were removed, forceps were used to pull apart the dorsal and ventral sides, then immediately fixed in 4% PFA for 1 hour. All steps following fixation were performed as described above. Confocal immunofluorescence of intact pinnae utilized the following antibodies: 1:50 Vδ4 (eFluor 600; clone GL2; 50–5702-80; eBioscience) and 1:200 Vγ5 (FITC; clone 536; 553229; BioLegend). To visualize free nerve endings in the whole skin, fixed skin was incubated with 1:100 anti-Tuj1-biotin (clone TuJ1; MAB1195; R&D Systems) overnight at 4°C. The next day, samples were incubated with 1:100 streptavidin-PE (405204; BioLegend). Fixation and washing of these samples were performed as described above. Imaging was performed on a LSM confocal microscope using ZEN Black v2.3, and processing was performed using Zen Blue v3.7 (Zeiss). The 3D tool generated an orthogonal projection of GD3 cells in contact with *Scn10a^{tdTomato}* free nerve endings.

To quantify the contact between epidermal γδ T cells and free nerve endings, images from *Scn10a^{tdTomato}* skin were analyzed. Using the orthogonal tool to account for the x-, y-, and z-axes, the number of times GD3 cells or DETCs came into direct contact were counted. Quantitative analysis of Tuj1 sensory nerve fiber density was performed using the HALO imaging analysis platform (Indica Labs). A strict positivity threshold was manually selected after reviewing each image. HALO's Area Quantification FL module was used to enumerate the percentage of the total area covered by pixels that reached this threshold, effectively characterizing the overall density of Tuj1 for each image.

Multiplex and ELISA Assay

Cell-free culture supernatant from unstimulated and stimulated γδ T cells, collected as described in the *Supernatant transfer and cytokine instillation* protocol, was assessed for secreted factors using the Mouse Cytokine/Chemokine 44-Plex Discovery Assay® Array (MD44; Eve Technologies). γδ T cell-free supernatant was tested for the presence of IL-3 or IL-17A using the BD OptEIA™ Mouse IL-3 ELISA Set (BD Biosciences) or IL-17A using the IL-17A ELISA MAX™ Deluxe ELISA Kit (BioLegend). In one experiment, cell-free

supernatant from stimulated skin immune cells, including sorted GD3 cells, αβ T cells, helper-like ILCs, and all remaining CD45$^+$ cells (other), was assayed for IL-3 as above. These immune populations were stimulated overnight with PMA (50 ng/mL)/Ionomycin (1 μg/mL). For all assays, the manufacturer's instructions were followed. ELISA samples were assessed on a SpectraMax iD5 microplate reader (Molecular Devices). Concentrations were determined from a standard curve.

Proliferation of DETCs and GD3 cells

To assess the viability of DETCs and GD3 cells following 5 days in culture, we isolated the cells following the *Supernatant transfer and cytokine instillation* protocol. Before plating, single-cell suspensions were incubated with 1:1000 CellTrace Violet (Thermo Fisher Scientific) at 37°C in 5% CO_2 for 20 minutes. 1:1 fully-supplemented RPMI was added for 5 minutes before pelleting and resuspension in the appropriate culture medium.

Overnight stimulation of MACS-enriched or FACS-sorted γδ T cells

Single-cell suspensions of mouse epidermis were prepared from *Skint1$^{-/-}$* Taconic FVB/N mice following the *Isolation of immune cells from mouse dermis and epidermis* protocol. These mice were selected for this protocol because the epidermal γδ T cell compartment lacks DETCs and contains high numbers of GD3 cells. Single-cell suspensions were enriched for γδ T cells following the TCRγδ$^+$ T Cell Isolation Kit, mouse (Miltenyi Biotec). Single-cell suspensions of mouse dermis and epidermis were prepared from WT or *Il3$^{GFPfl/fl}$* mice following the *Isolation of immune cells from mouse dermis and epidermis* protocol. Dermal γδ T cells, DETCs, and GD3 cells were then FACS-sorted.

15,000 MACS-enriched GD3 cells or 4,000 FACS-sorted γδ T cells were plated in a tissue-culture-treated flat-bottom 96-well plate and stimulated with papain (5 μg/mL), PMA (50 ng/mL)/Ionomycin (1 μg/mL), or Dynabeads Mouse T-Activator CD3/CD28 beads (Gibco) at a bead-to-cell ratio of 5:1. Following overnight incubation at 37°C in 5% CO_2, cells were incubated with fluorescent-conjugated antibodies in FACS Buffer for 15 minutes at 4°C, then fixed with 4% PFA for 8 minutes at room temperature. Fluorescent-conjugated antibodies targeting intracellular cytokines were added to each well in 1x eBioscience™ Permeabilization Buffer (Invitrogen) for 1 hour at 4°C. Cells were washed twice with DPBS and then assessed by flow cytometry.

Quantitative PCR (QPCR)

Dermal γδ T cells, DETCs, and GD3 cells were FACS isolated, and RNA was extracted using the QIAGEN RNeasy Micro Kit in accordance with the manufacturer's protocol. 50 μL of cDNA per reaction was generated using random hexamers, Oligo (dT), magnesium chloride, dNTPs (10 mM), Reverse Transcriptase, and RNase inhibitor (all from Thermo Fisher Scientific). Gene expression was measured using a LightCycler 96 Real-Time PCR System (Roche) and SYBR Green Master Mix (Roche) reagents. The reaction cycles were: 95°C for 600 s, then 95°C, 60°C, and 72°C for 10 s each for 45 total cycles, followed by 95°C for 10 s, 65°C 20 for 60 s, and finally 97°C for 1 s. Fluorescence was quantified

during each amplification. LightCycler 96 Software 1.1 (Roche) was used to determine quantification cycle (Cq) values for each cell type. Cq values of *Il3* were divided from *Gapdh* to determine the ratio of copies per Gapdh. The *Gapdh* primers were: forward 5' TTG ATG GCA ACA ATC TCC AC 3' and reverse 5' CGT CCC GTA GAC AAA ATG GT 3'. The *Il3* primers were: forward 5' GCC TGC CTA CAT CTG CGA AT 3' and reverse 5' GGT TAG GAG AGA CGG AGC CA 3'.

RNA fluorescence in situ hybridization (RNA ISH) of mouse DRGs

Tissue preparation

All materials and reagents were RNAase-free. WT DRGs were carefully removed and placed in OCT Compound, then snap-frozen on dry ice within 5 minutes of collection. Tissue blocks were stored at −80°C and used within 3 months. Frozen tissue blocks were equilibrated to −20°C inside a Leica Jung Frigocut 2800E cryostat (Leica Biosystems) for 1 hour. 10 μm tissue sections were cut onto SuperFrost Plus Microscope Slides (Fisher Scientific) and kept at −20°C for 1 hour to enhance tissue adherence, then stored at −80°C and used within 3 months.

RNAScope reagents (ACDBio) were used to prepare DRG tissue sections for RNA ISH. In brief, sections were removed from storage and placed in pre-chilled 4% paraformaldehyde (Electron Microscopy Sciences) at 4°C for 1 hour. Sections were rinsed twice in 1x DPBS and, then serially dehydrated in 50%, 70%, 100%, and 100% EtOH (Decon Labs) for 5 minutes each. Slides were dried for 10 minutes, and an ImmEdge pen (Vector Laboratories) was used to create a hydrophobic barrier around the tissue section. Tissue sections were incubated in H_2O_2 for 10 minutes and washed twice with H_2O. Tissue sections were incubated in Protease IV for 10 minutes and washed twice with H_2O. Following these steps to prepare tissue sections for probe hybridization, the manufacturer's instructions were followed. To determine whether *Il3ra* transcript was enriched within specific neuronal subsets, we paired *Il3ra* detection with that for marker genes of the NP1 (*Gfra1*, *Trpc3*), NP2 (*Gfra1*), NP3 (*Sst*), PEP1 (*Gal*), PEP2 (*Asic3*), and cold (*Trpm8*) sensory neuronal subsets previously identified by scRNAseq[33–36]. To determine whether *Tac1* transcript levels were decreased in the absence of sensory neuronal *Il3ra*, we paired *Tac1* with *Trpv1*. Probes were visualized by pairing with the following fluorescent probes: TSA vivid 520 was 1:750, TSA vivid 570 was 1:1500, TSA vivid 650 was 1:1500, and TSA-DIG (1:3000) was paired with Opal Polaris 780 (1:1000; Akoya Biosciences). Fluorophore concentrations were optimized to balance the signal intensity of each channel. Glass coverslips were mounted on microscope slides with Prolong Diamond Antifade Mountant (Thermo Fisher Scientific).

Image acquisition

Images of tissue slides were acquired on an Akoya PhenoImager HT multi-spectral slide scanner (Akoya Biosciences) at 20x (0.5 microns per pixel) resolution. Exposures were set for each image individually to avoid saturation or underexposure. Akoya Biosciences inForm v2.7.1 software was used to spectrally separate signals from each fluorophore and to mitigate the effect of native tissue autofluorescence. The spectral library was created using the synthetic Opal spectra and autofluorescence spectra from unstained mouse DRG

tissue. Unmixed tiles produced by inForm were fused to reproduce a whole-slide pyramidal TIF using Indica Labs HALO software v3.6. In *Tac1* experiments, images of tissue slides were acquired with ZEN Blue v3.7 on a Zeiss Axio Imager M2 Upright Microscope at 20x resolution. Exposures were set for each image individually to avoid saturation or underexposure.

Image analysis

Quantitative image analysis was performed using the HALO image analysis platform from Indica Labs. To minimize potential bias in data analysis, we utilized an artificial intelligence/machine learning approach to annotate 987 individual DRG neurons based on the expression of sensory neuronal subset marker genes, and then quantitated *Il3ra* copies per neuron. In *Tac1* experiments, we annotated 925 individual DRG neurons. Areas of interest containing in-focus DRG tissue sections were manually annotated. Cell detection and segmentation were performed using two HALO-AI v3.6 artificial neural network classifiers, one per staining panel. Each segmentation network was trained on datasets of 150 hand-annotated cells per panel until segmentation results were stable and sufficiently accurate. The segmentation networks were trained at the whole-cell level using a weighted average of the stains that were diffuse and spread across the cell body, which were all stains except *Il3ra*, to properly detect cell boundaries. Two HALO AI Object Phenotyper artificial neural networks were then trained to classify the cells into neuronal phenotypes of interest per staining panel. The training sets for the phenotyper networks consisted of the same cells used to train the segmentation networks. After cells were detected and phenotyped using both neural network classifiers, each staining channel was quantified per cell using the HALO FISH-IF v2.2.5 module. The number of *Il3ra* ISH copies per cell was determined based on the size and intensity of detected dots. The fluorescence intensity of *Tac1* in *Tac1*+*Trpv1*+ and *Tac1*+*Trvp1*- cells was determined.

Calcium imaging of dorsal root ganglia neurons

20 μL of Poly-D-Lysine & Laminin solution (Millipore Sigma) was pipetted as a small dot on a Fluorodish cell culture petri dish (World Precision Instruments). Fluorodishes were then incubated at 37°C in 5% CO_2 for 2 hours to coat the dot's location with Poly-D-Lysine & Laminin. DRGs were harvested and dissociated as described in the *Isolation of cells from mouse dorsal root ganglia* protocol. 10 μL of cells (at 5 μL per DRG harvested) was plated at the exact spot of the Poly-D-Lysine & Laminin dot on the Fluorodishes. Dishes were incubated at 37°C in 5% CO_2 for 2 hours. After DRG neurons attached to the Poly-D-Lysine & Laminin-coated Fluorodish, plates were flooded with 1 mL of supplemented NBM. Fluorodishes were incubated overnight at 37°C in 5% CO_2. The following day, the medium was aspirated and replaced with supplemented NBM containing 5 mM of the calcium indicator dye Fura-2 (Invitrogen). In some experiments, 5 μg/mL IL-3 was added during this step. Fluorodishes were returned to 37°C in 5% CO_2 for 30 minutes. Fluorodishes were washed three times with Krebs-Ringer Solution (Alfa Aesar) before the plate was completely flooded with Krebs-Ringer Solution. Krebs-Ringer solution contained 20 mM sodium chloride, 5 mM potassium chloride, 2 mM calcium chloride, 1 mM magnesium chloride, 25 mM sodium bicarbonate, and 5.5 mM D-glucose, pH 7.3.

The ValveBank®8 Pinch Valve Perfusion System (AutoMate Scientific, Inc) was used in calcium imaging experiments to perfuse cells. The perfusion pencil was held in a PatchStar Micromanipulator (Scientifica). Fluorodishes were placed on an Inverted Motorised Movable Top Plate with a petri dish/slide adaptor ring (Scientifica) that was placed over a Nikon Ti2-A Intelligent Inverted Microscope (Nikon Instruments). Fura-2-loaded DRG neurons were illuminated every second with alternating 340 and 380 nm wavelengths produced by a RETRA FURA III light engine (Lumencor). Images were captured with a pco.edge 4.2 LT sCMOS Camera (PCO). Ratiometric assessment of 340/380 signals was performed with NIS-Elements v5.30.02 (Nikon Instruments). DRG neurons were identified by drawing a region of interest around each cell. Neurons were considered live and excitable if they responded to capsaicin, AITC, or KCl with a 15% ratio increase from baseline. IL-3 and papain excited neurons if their perfusion led to a 15% ratio increase from baseline.

In sequential stimuli experiments, Fura-2-loaded DRG neurons were perfused with Krebs-Ringer solution, followed by 5 μg/mL recombinant-mouse IL-3, 1 μg/mL papain, 0.5 μM capsaicin, 200 μM AITC (Millipore Sigma), and 40 mM KCl (Millipore Sigma). Between each stimulus, Krebs-Ringer solution was perfused through the system. The percent of neurons that responded to IL-3, papain, AITC, or capsaicin were plotted as a proportion of total live and excitable neurons. In priming experiments, control DPBS or 5 μg/mL IL-3 was added to the Neurobasal™-A-Fura-2 mixture. Fura-2-loaded, DPBS or IL-3 primed DRG neurons were perfused sequentially with Krebs-Ringer solution, followed by increasing doses of papain (100, 250, and 1,000 μg/mL), capsaicin, AITC, and KCl. The percent of neurons that responded to the increasing doses of papain were plotted as a proportion of total live and excitable DRG neurons.

Dorsal root ganglia neuron ex vivo culture

40 μL of Poly-D-Lysine & Laminin solution (Millipore Sigma) was pipetted in a tissue-culture-treated flat-bottom 96-well plate (Corning) and incubated for 2 hours before washing 4x with DPBS. DRGs were harvested and dissociated as described in the *Isolation of immune cells from mouse dorsal root ganglia* protocol. 10,000 DRG neurons/well were cultured for 7 days in supplemented NBM containing 25 ng/mL NGF (Alomone Labs), 2 ng/mL GDNF (Peprotech), and Cytosine β-D-arabinofuranoside hydrochloride (Millipore Sigma). In the indicated experiments, 500 nM fedratinib or 100 μM STAT5-IN-1 was added to wells on day 2, while 2.5 μg/mL IL-3 was added on day 6. Experiments were performed on day 7.

STAT5 phosphorylation in dorsal root ganglia neurons

Glass coverslips were treated with 20 μL of Poly-D-Lysine & Laminin solution (Millipore Sigma) and incubated for 2 hours before washing 4x with DPBS. Sensory neurons were prepared following the *Dorsal root ganglia neuron* ex vivo *culture* protocol, but cultured overnight on a glass coverslip in 400 μL supplemented NBM. Fedratinib was added to the overnight culture medium when indicated. The following day, cells were treated with 2.5 μg/mL IL-3 or DPBS for 5 minutes, then fixed for 5 minutes with ice-cold 4% PFA.

The fixed neurons were washed 3x with DPBS for 10 minutes each time, then incubated overnight at 4°C in 1.715 μg/mL anti-pSTAT5 (Cell Signaling Technology) and 1:300 Neurotrace 435/455 (Thermo Fisher Scientific). The following day, cells were washed 3x with DPBS for 10 minutes each time, then incubated in 0.483 mg/mL of fluorescently-conjugated goat anti-rabbit IgG (Abcam) for 2 hours at room temperature. After washing the cells 4x with DPBS for 10 minutes each time, glass coverslips were mounted on microscope slides with Prolong Diamond Antifade Mountant (Thermo Fisher Scientific). Images of slides were acquired on a Zeiss Axio Imager M2 Upright Microscope at 20x resolution. Exposures were set to avoid saturation or underexposure. Images were assessed in FIJI v2.14.0 to identify neurotrace^{+} neurons. Images were converted to 32-bit grayscale, and then regions of interest (ROIs) of neurotrace^{+} cells were determined using the intensity of neurotrace and cell morphology. ROIs were applied to the pSTAT5 channel images, and then the intensity of pSTAT5 fluorescence was measured. Cells were considered pSTAT5[+] using a threshold that corresponded to the negative control.

Chromatin Immunoprecipitation (ChIP) assay

We evaluated the *Tac1* promoter region and identified a putative STAT5 binding site using the Eukaryotic Promoter Database (p<0.001). We prepared sensory neurons following the *Dorsal root ganglia neuron* ex vivo *culture* protocol and plated 200,000 cells/well in a 12-well plate. The Abcam[TM] High-Sensitivity ChIP Kit (ab185913) (Abcam) was used, and the manufacturer's instructions were followed. 100 μL of chromatin lysate was sonicated at 190 watts for 30, 5-minute cycles, with 15 seconds on and 30 seconds off (Qsonica). DNA associated with *Tac1* was precipitated using anti-STAT5 (R&D Systems), with anti-IgG as a control (included in ChIP Kit). Following precipitation of DNA associated with STAT5, QPCR primers were designed to target the specific region of the *Tac1* promoter with a predicted STAT5 binding site: forward 5' ACC GTG GTT TGC TAA AGA CT 3' and reverse 5' TTA AGC CTT GTT GGA GGG CT 3'.

Substance P release from dorsal root ganglia neurons

We prepared sensory neurons following the *Dorsal root ganglia neuron* ex vivo *culture* protocol. On day 7, the media was replaced with supplemented NBM for 10 minutes. This supernatant was considered 'unstimulated.' 5 μg/mL (low-dose) papain in supplemented NBM was then added to the wells for 10 minutes. This supernatant was considered 'stimulated.' 5 μg/mL (low-dose) papain was selected because it caused limited (non-significant) release of substance P in the absence of IL-3 priming. Cell-free supernatant was assayed for substance P using the Substance P ELISA Kit (Cayman Chemical), and the data were analyzed following the manufacturer's instructions. To control for the nonspecific effects of papain on the ELISA assay, we included 'no cells control' wells that were unstimulated or stimulated with papain as described. No cell control concentrations were subtracted (corrected) from wells containing cells.

Statistical methods

Results are displayed as follows: violin plots show the median and quartiles, while bar plots, dose-response curves, and time-courses are mean ± SEM. Symbols represent individual wells, experimental replicates, or mice, or as described in figure legends. Unless otherwise noted, data were processed in Excel v16.86 and statistical analyses were performed using Prism 10 (GraphPad). Data were assessed for normality by the following tests: D'Agostino & Pearson test, Anderson-Darling test, Shapiro-Wilk test, and Kolmogorov-Smirnov test. When two or more normality tests indicated that the distribution of data was not normal, the appropriate nonparametric test was performed. When comparing one variable among three or more groups or two variables, ANOVA was always used as it is robust to violations of normality. As indicated in figure legends, Two-sided *t*-tests, Two-sided Mann Whitney *U*-tests, One-way ANOVA with Tukey's multiple comparisons tests, Two-way ANOVA with Tukey's multiple comparisons (comparing all groups), or Two-way repeated measures ANOVA (with paired data) were used throughout the study. Paired analyses were used when samples were derived from the same subject. Data were significant if they met the following p-value criteria: * $p<0.05$, ** $p<0.01$, *** $p<0.001$, **** $p<0.0001$, ns=not significant.
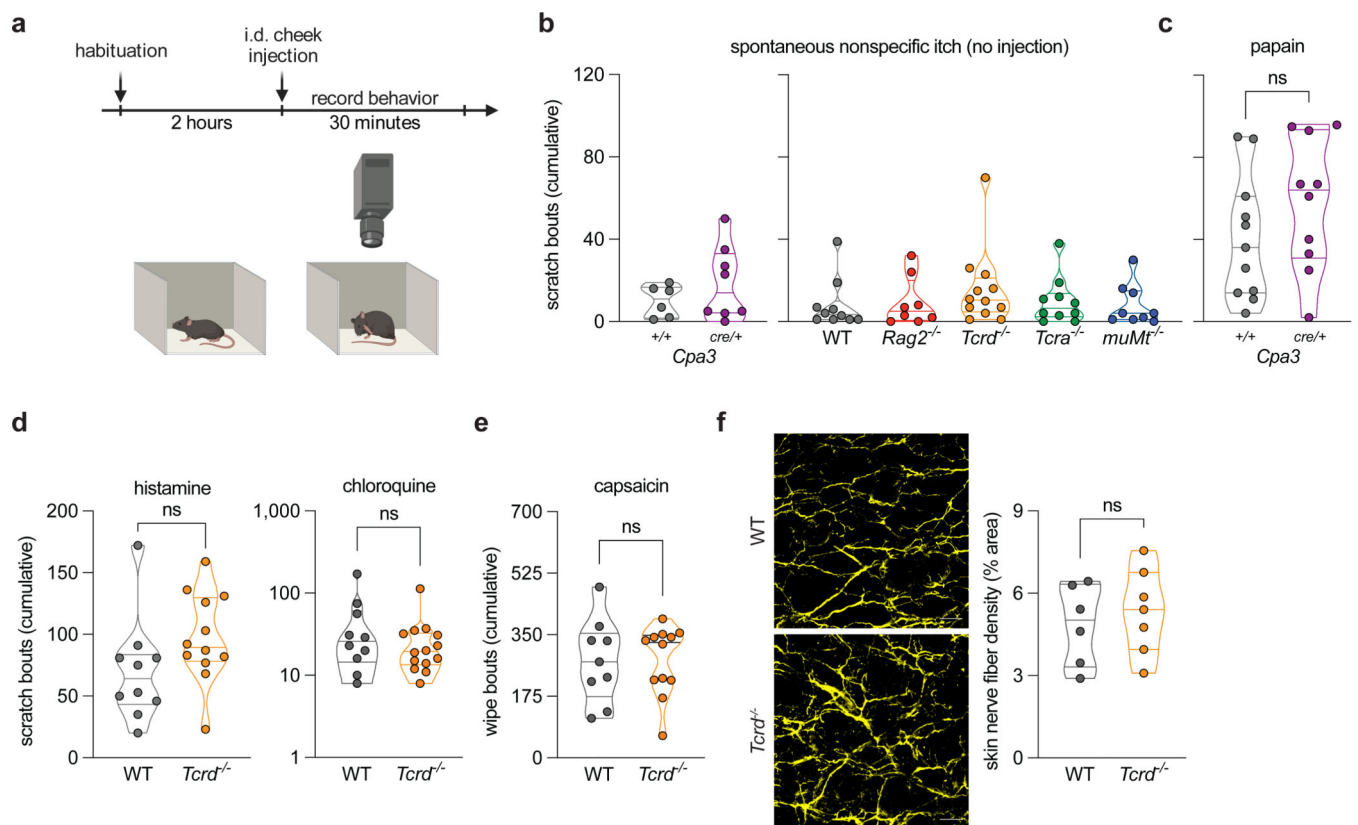
Extended Data

Extended Data Figure 1. Mice lacking γδ T cells have no broad defect in itch, pain, or neuronal innervation in the skin.

a, Schematic of standard behavior protocol. **b**, Cumulative spontaneous nonspecific scratch at any skin site (n=6 $Cpa3^{+/+}$; n=8 $Cpa3^{cre/+}$; n=10 WT; n=8 $Rag2^{-/-}$; n=12 $Tcrd^{-/-}$; n=10 $Tcra^{-/-}$; n=9 $muMT^{-/-}$). **c-e**, Cumulative cheek scratch bouts following intradermal (i.d.) injection as indicated (**c**: n=11 $Cpa3^{+/+}$; n=10 $Cpa3^{cre/+}$; **d**, histamine: n=10 WT; n=12 $Tcrd^{-/-}$; **d**, chloroquine: n=10 WT; n=14 $Tcrd^{-/-}$; **e**: n=9 WT; n=12 $Tcrd^{-/-}$). **f**, Confocal microscopy z-stack of Tuj1 in naïve WT and $Tcrd^{-/-}$ mice. The scale bar is 50 µm (n=6 WT; n=7 $Tcrd^{-/-}$). Symbols represent individual mice (**b-e**) or images (**f**). Violin plots show the median and quartiles. Data represent at least two independent experiments and were combined. Statistical tests: One-way ANOVA with Tukey's multiple comparisons test (**b**, WT v indicated mouse strains), Two-sided unpaired t-test (**b**, $Cpa3$; **c**; **d**, histamine; **e-f**), or Two-sided Mann Whitney U-test (**d**, chloroquine). ns=not significant.
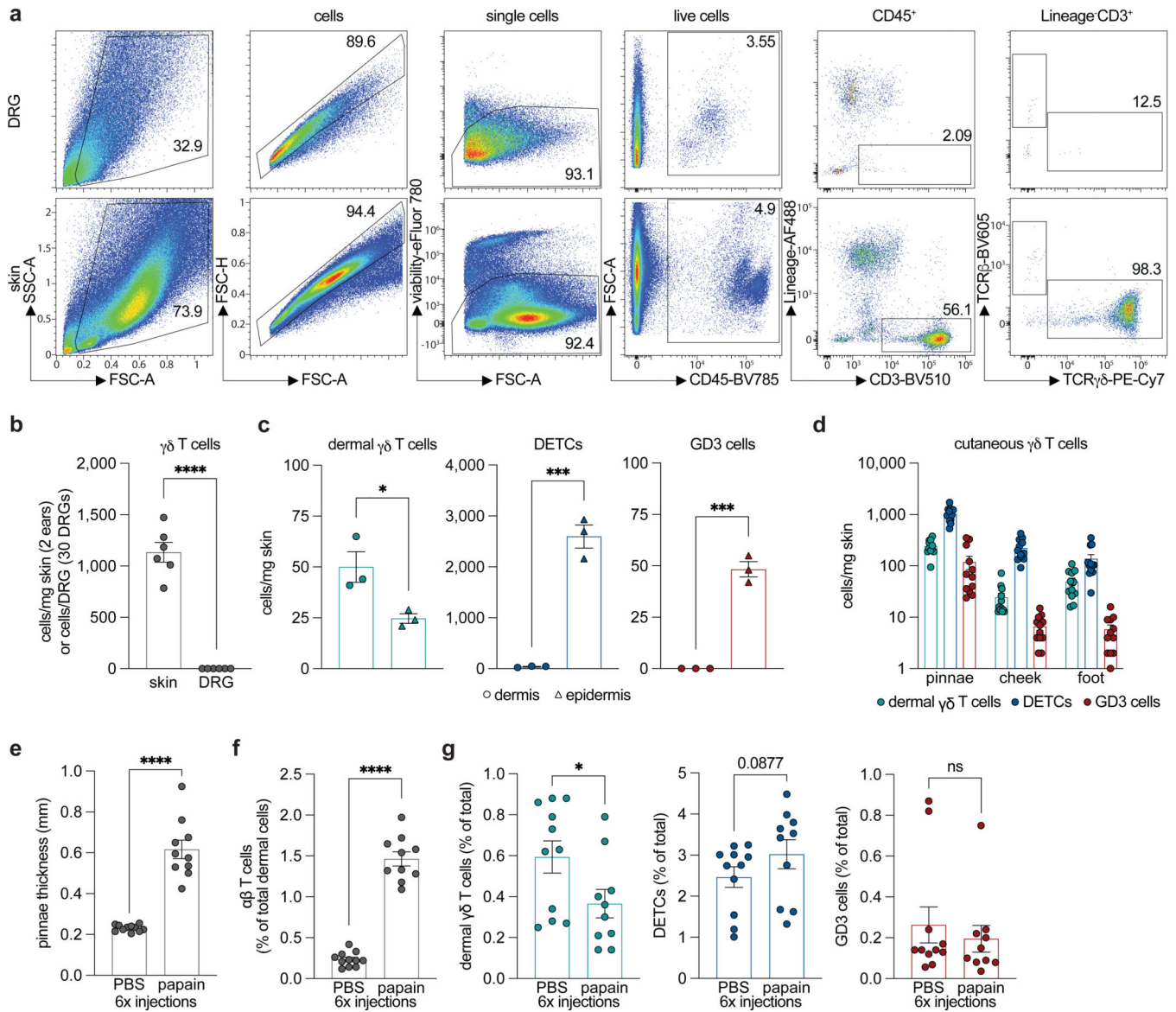
Extended Data Figure 2. GD3 cells are Vγ5⁻ epidermal γδ T cells.

a, Flow cytometry of naïve WT pinnae or dorsal root ganglia (DRG). **b-d**, **f-g**, Flow cytometric quantification of naïve WT pinnae or DRG (**b**), naïve WT dermis or epidermis (**c**), naïve WT pinnae, cheek, or foot (**d**), or WT pinnae (**g**) (**b**: n=6 per group; c: n=3 per group; **d**: n=12 per group; **f-g**: n=11 PBS; n=10 papain). **e,** Pinnae thickness was measured following chronic papain exposure (n=11 PBS; n=10 papain). Symbols represent individual mice. Bar plots are mean ± SEM. Data represent at least two independent experiments and were combined, except in **c**. Statistical tests: Two-sided unpaired *t*-test (**b-f**; **g**, dermal γδ T cells) or Two-sided Mann Whitney *U*-test (**g**, DETCs and GD3 cells). * p<0.05, *** p<0.001, **** p<0.0001, ns=not significant.
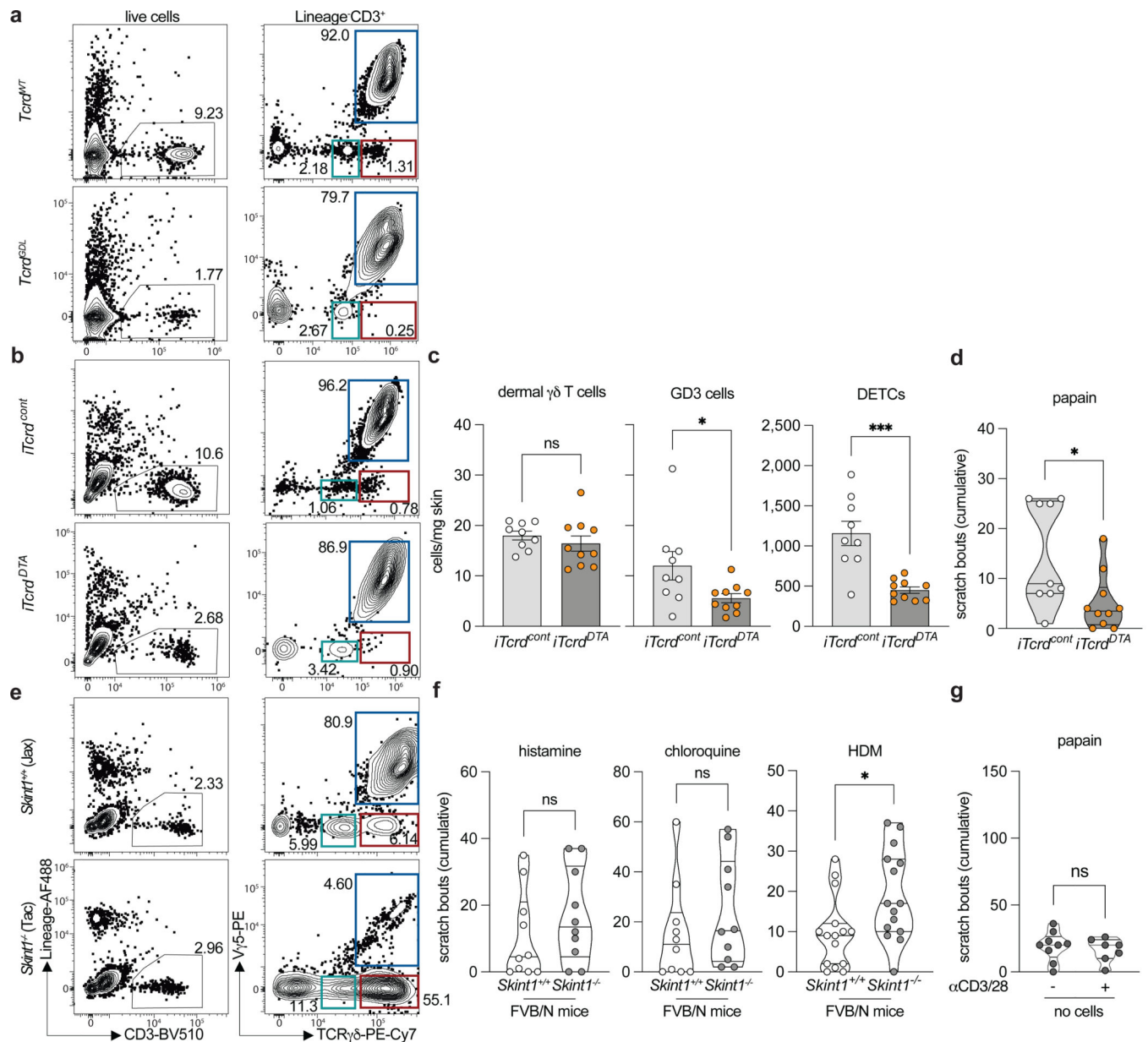
Extended Data Figure 3. Dermal γδ T cells and DETCs are not required for allergic itch.

a-b, **e**, Flow cytometry of naïve pinnae [**a** gating strategy corresponding to Figure 1d; **e** gating strategy corresponding to Figure 1f]. **c**, Flow cytometric quantification of naïve WT pinnae (n=9 *iTcrd*^{cont}; n=10 *iTcrd*^{DTA}). **d**, **f-g**, Cumulative cheek scratch bouts following i.d. injection as indicated (**d**: n=9 *iTcrd*^{cont}; n=10 *iTcrd*^{DTA}; **f**: n=10 histamine and chloroquine; n=15 HDM; **g**: n=9 αCD3/28 - ; n=7 αCD3/28 +). Symbols represent individual mice. Bar plots are mean ± SEM. Data represent at least two independent experiments and were combined. Statistical tests: Two-sided unpaired *t*-test (**c**, **g**) or Two-sided Mann Whitney *U*-test (**d**, **f**). * p<0.05, *** p<0.001, ns=not significant.
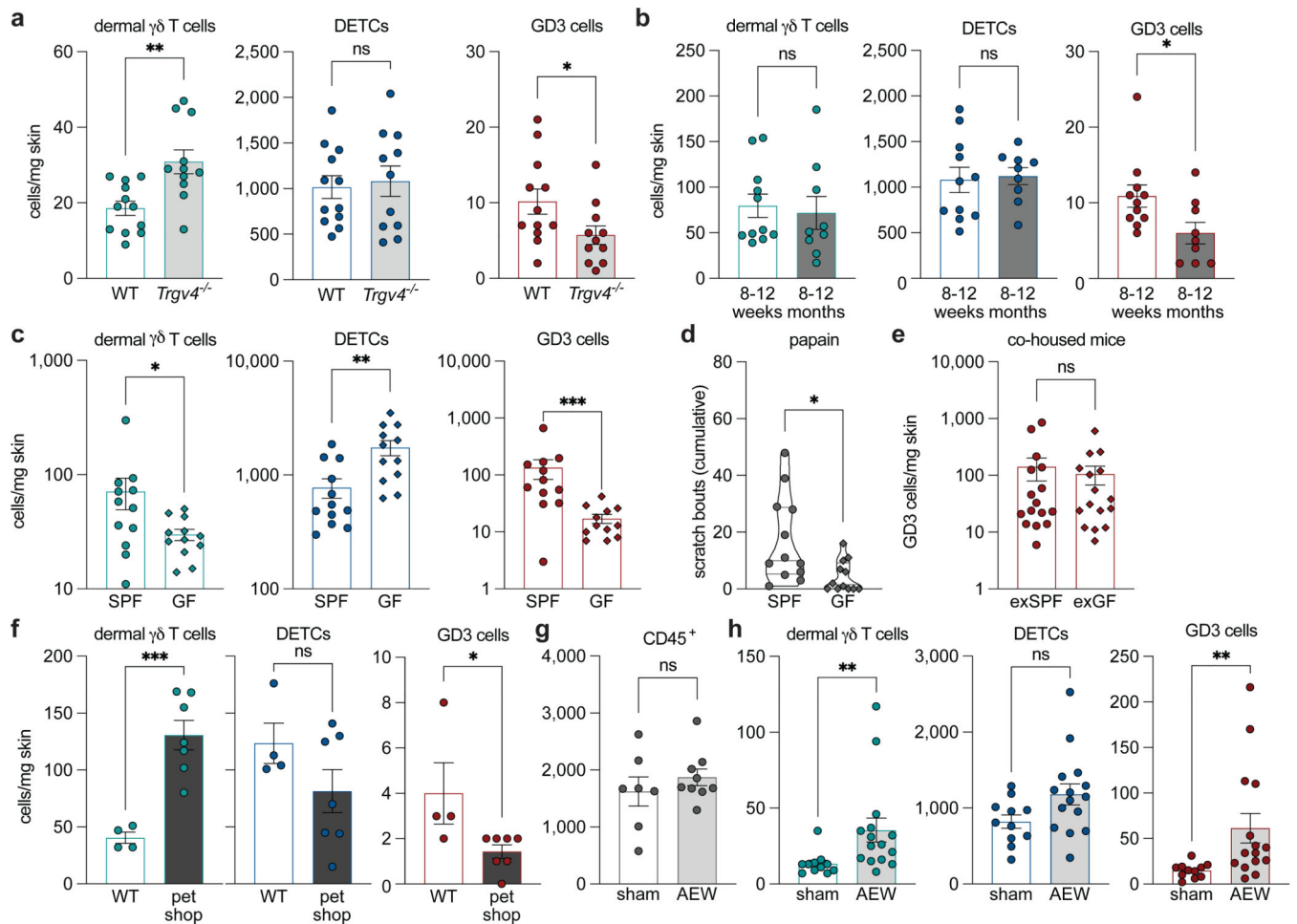
Extended Data Figure 4. GD3 cells are regulated by *Trgv4*, age, microbial factors, and dry skin.
a-c, **e-h**, Flow cytometric quantification from pinnae (**a**: n=12 WT; n=11 *Trgv4*^{-/-}; **b**: n=11 8–12 weeks; n=9 8–12 months; **c**: n=12 per group; **e**: n=16 per group; **f**: n=4 WT; n=7 per shop; **g**: n=7 sham; n=9 AEW; **h**: n=11 sham; n=15 AEW). **d**, Cumulative cheek scratch bouts following i.d. injection of papain (n=12 per group). Symbols represent individual mice. Bar plots are the mean ± SEM. Violin plots show the median and quartiles. Data represent at least two independent experiments and were combined, except in **f**. Statistical tests: Two-sided unpaired *t*-test (**a**; **b**, DETCs; **f**, dermal γδ T cells and DETCs; **g**; **h**, DETCs) or Two-sided Mann-Whitney *U*-test (**b**, dermal γδ T cells and GD3 cells; **c-e**; **f**,

GD3 cells; **h**, dermal γδ T cells and GD3 cells). * p<0.05, ** p<0.01, *** p<0.001, ns=not significant.
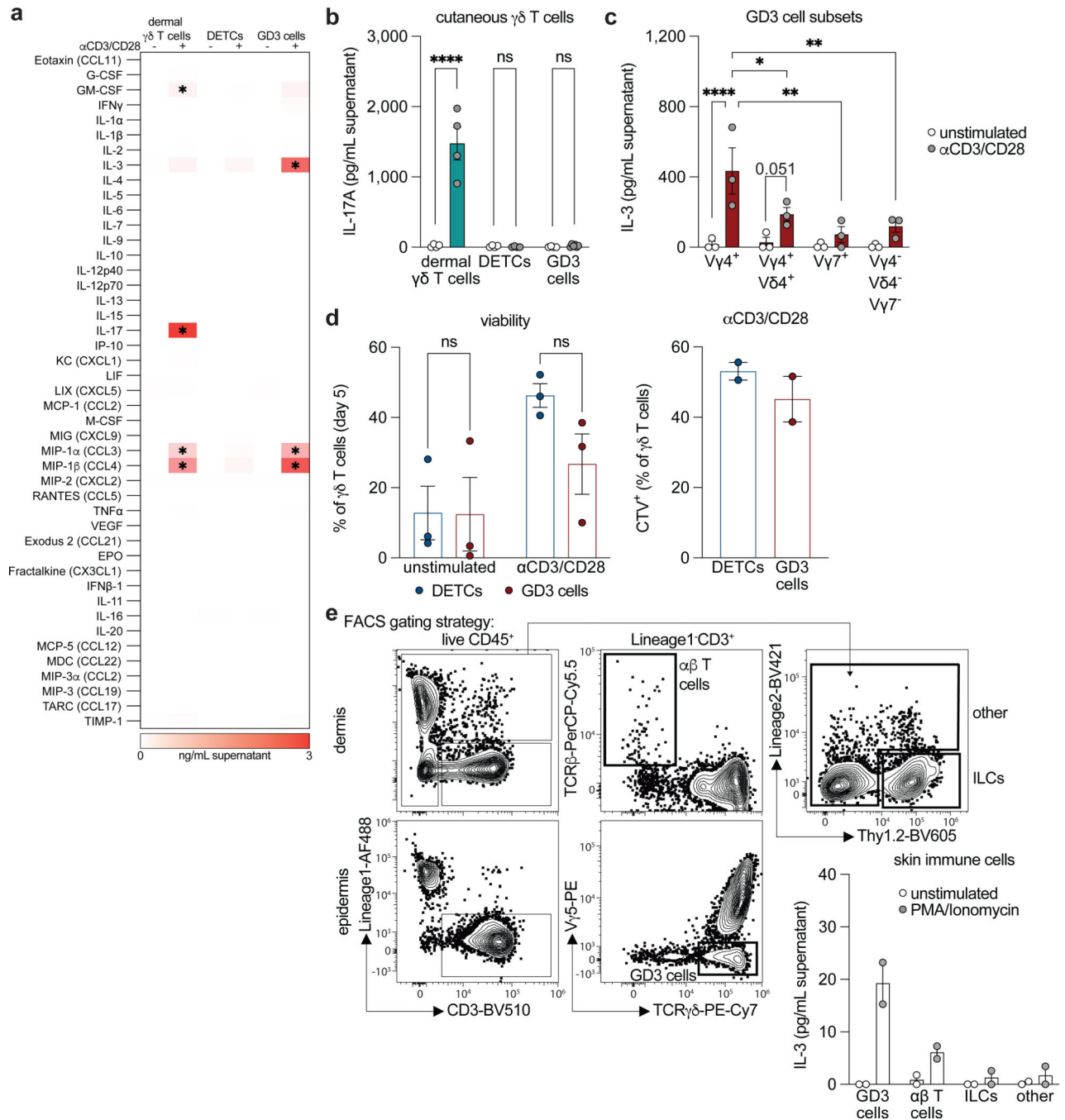
**Extended Data Figure 5. Vγ4⁺ GD3 cells are the major source of IL-3 in naïve skin.**
a, Heatmap of multiplex assay of cell-free supernatant from FACS sorted γδ T cells stimulated as indicated (n=3 per group). * symbols represent a cytokine or chemokine that significantly increased following stimulation. **b-c**, **e**, IL-17A or IL-3 ELISA of cell-free supernatant from FACS sorted γδ T cells or immune cells stimulated as indicated [**b**: n=4

per group, except stimulated GD3 cells (n=6); **c**: n=3 per group; **e**: n=2 per group]. **d**, Flow cytometry of FACS isolated γδ T cells. CTV = cell trace violet (viability: n=3 per group; CTV: n=2 per group). Symbols represent individual wells (**b**) or experimental replicates (**c-e**). Bar plots are mean ± SEM. Data represent at least two independent experiments combined, except in **a**, a single pilot experiment, and **b**, a representative experiment with n=4–6 wells. Statistical tests: Two-way ANOVA with Tukey's multiple comparisons test (**a-c**) or Two-way ANOVA (**d**, viability). * $p<0.05$, ** $p<0.01$, **** $p<0.0001$, ns=not significant.
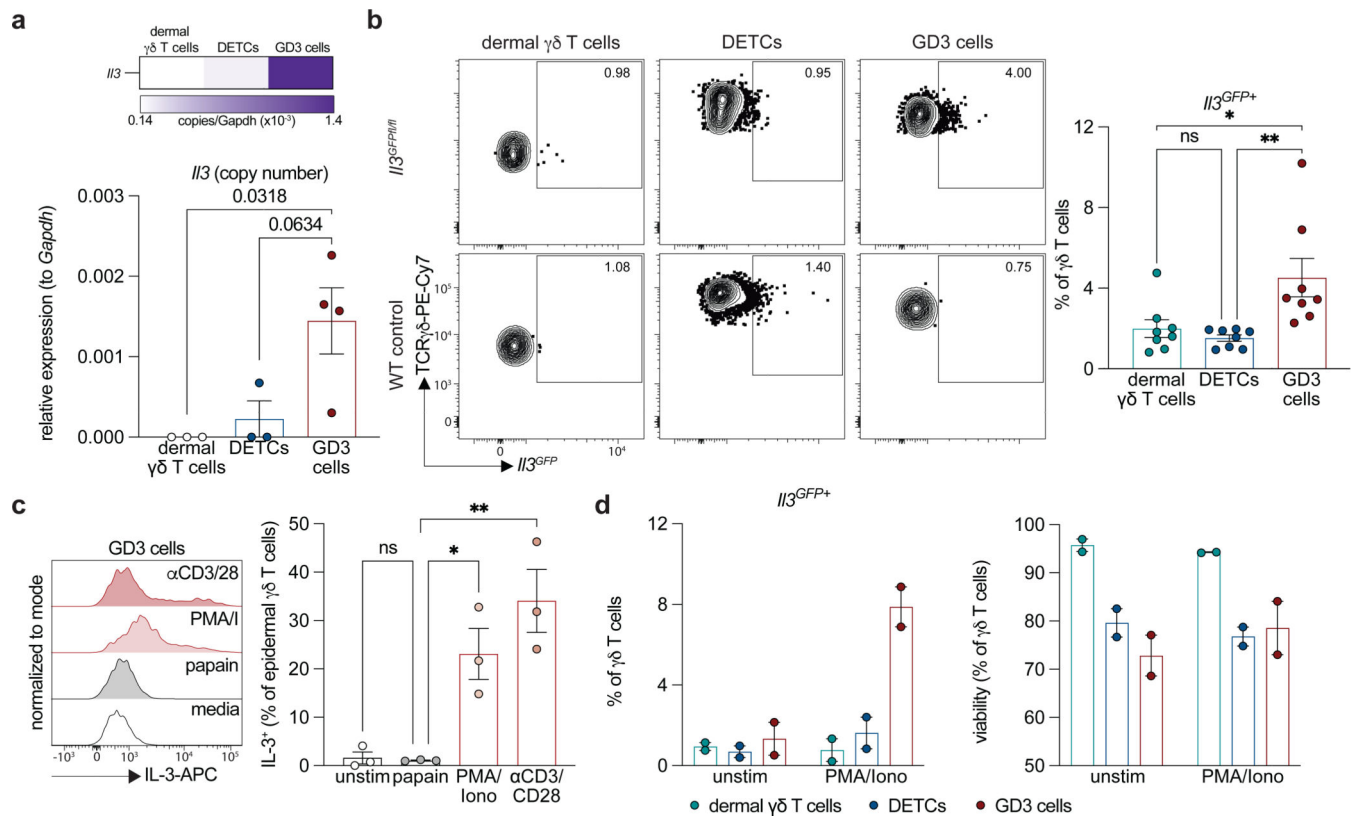
Extended Data Figure 6. Expression and production of IL-3 by GD3 cells.
a, QPCR of *Il3* (normalized to *Gapdh*) from FACS sorted γδ T cells from naïve WT pinnae [n=3 per group, except GD3 cells (n=4)]. **b**, Flow cytometric quantification of naïve *Il3^GFPfl/fl* pinnae (n=8 per group). **c-d**, Flow cytometric quantification of MACS enriched GD3 cells from *Skint1^-/-* FVB/N pinnae (**c**) or FACS sorted γδ T cells from *Il3^GFPfl/fl* pinnae (**d**) left unstimulated (unstim) or stimulated as indicated (**c**: n=3 per group; **d**: n=2 per group). Symbols represent individual experimental replicates of pooled mice (**a**, **c-d**) or mice (**b**). Bar plots are mean ± SEM. Data represent at least two independent experiments and were combined. n=3–4 experimental replicates of pooled mice (**a**), n=8 mice (**b**), or n=2–3 experimental replicates (**c-d**). Statistical tests: One-way ANOVA with Tukey's multiple comparisons test (**a-c**). * $p<0.05$, ** $p<0.01$, ns=not significant.
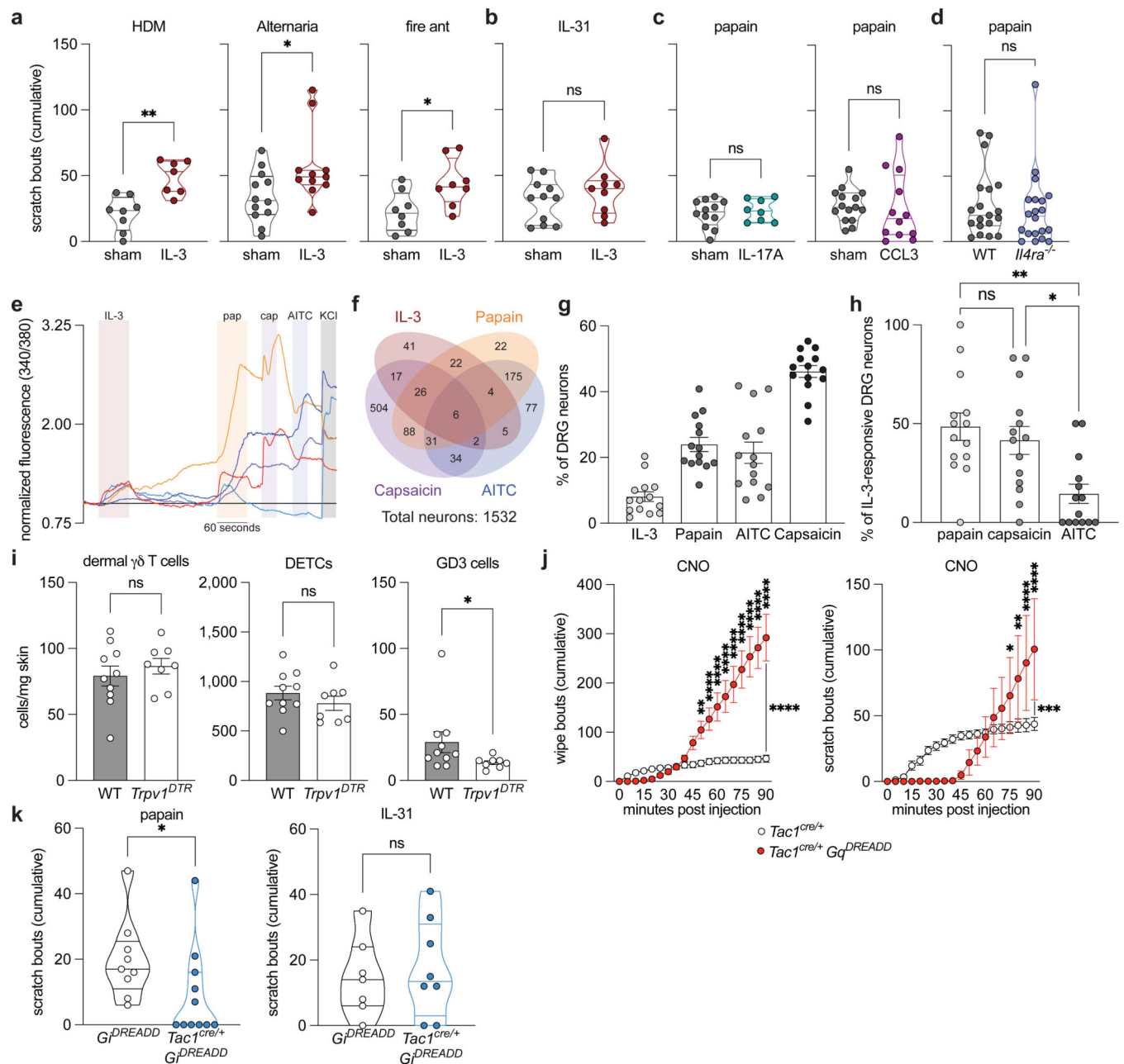
Extended Data Figure 7. IL-3 targets PEP1 sensory neurons, which encode mixed itch and pain and are required for allergic itch.

a-c, Cumulative cheek scratch bouts following i.d. injection of recombinant cytokine, then allergen or IL-31 (**a**: n=8 HDM sham; n=7 HDM IL-3; n=12 *Alternaria* sham; n=11 *Alternaria* IL-3; n=8 fire ant; **b**: n=11 sham; n=9 IL-3; **c**: n=12 papain sham; n=8 papain IL-17A; n=15 papain sham; n=12 papain CCL3). **d**, Cumulative cheek scratch bouts following i.d. injection of papain (n=19 WT; n=20 *Il4ra*^{−/−}). **e**, Representative traces of ratiometric calcium imaging of DRG neurons sequentially stimulated as indicated. **f**, Venn diagram indicating the overlapping responsiveness of individual DRG neurons. **g**, Percent of DRG neurons that responded to the indicated stimuli (n=14 per group). **h**, Percent of

IL-3 responsive DRG neurons that also responded to papain, capsaicin, or AITC (n=14 per group). **i**, Flow cytometric quantification of naïve pinnae (n=10 WT; n=8 $Trpv1^{DTR}$). **j**, Cumulative cheek wipe or scratch bouts following i.d. injection of CNO (n=10 $Tac1^{cre/+}$; n=8 $Tac1^{cre/+}Gq^{DREADD}$). **k**, Cumulative cheek wipe or scratch bouts following i.d. injection of CNO, then papain or IL-31 (n=9 Gi^{DREADD} papain; n=11 $Tac1^{cre/+}Gi^{DREADD}$ papain; n=7 Gi^{DREADD} IL-31; n=8 $Tac1^{cre/+}Gi^{DREADD}$ IL-31). Symbols represent mice (**a-d**, **i**, **k**) or individual wells **(g-h)**. Violin plots show the median and quartiles. Bar plots and time courses are mean ± SEM. Data represent at least two independent experiments and were combined. Statistical tests: Two-sided unpaired *t*-test (**a**, HDM and fire ant; **b-c**; **i**, dermal γδ T cells and DETCs; **k**, IL-31), Two-sided Mann Whitney *U*-test (**a**, Alternaria; **d**; **i**; GD3 cells; **k**, papain), One-way ANOVA with Tukey's multiple comparisons test (**h**), or Two-way ANOVA with Tukey's multiple comparisons test (**j**). * p<0.05, ** p<0.01, *** p<0.001, **** p<0.0001, ns=not significant.
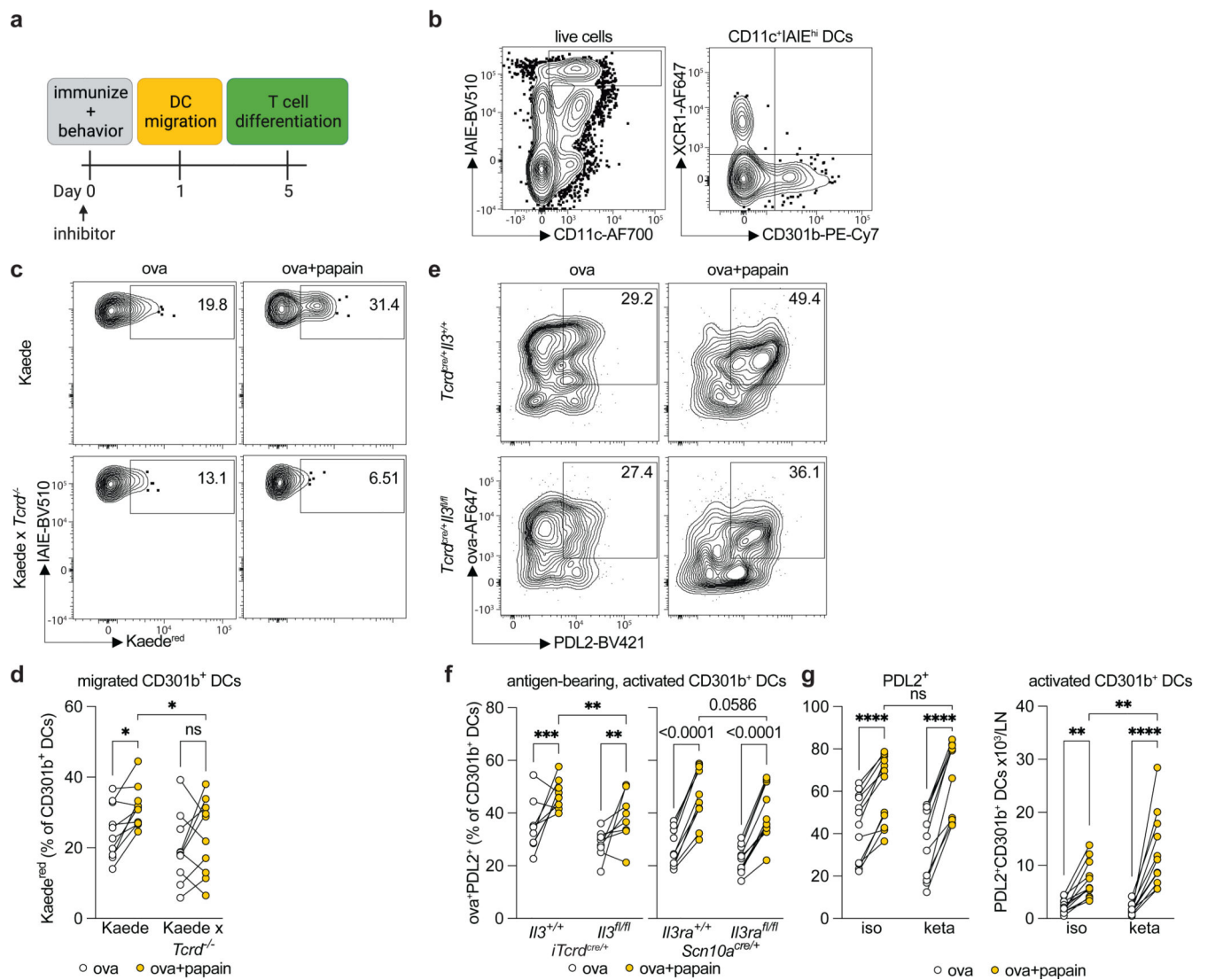
Extended Data Figure 8. The absence of the GD3-IL-3-sensory neuron axis inhibits papain-induced Th2-skewing dendritic cell migration.

a, Schematic of the allergic immune response protocol. **b-c**, **e**, Flow cytometry of the draining lymph node (dLN) 24 hours after immunization with ova±papain (gating strategy corresponding to Figure 4a–b, i, k). **d**, **f-g**, Flow cytometric quantification of the draining lymph node (dLN) 24 hours after immunization with ova±papain (**d**: n=10 per group; **f**: n=12 $iTcrd^{cre/+}Il3^{+/+}$; n=11 $iTcrd^{cre/+}Il3^{fl/fl}$; n=10 $Scn10a^{cre/+}Il3ra^{+/+}$; n=11 $Scn10a^{cre/+}Il3ra^{fl/fl}$; **g**: n=12 iso; n=11 keta). Symbols represent individual mice. Symbols connected by lines indicate paired samples derived from the same mouse. Data represent at least two independent experiments and were combined. Statistical tests: Two-way repeated measures ANOVA (**d**, **f-g**). * p<0.05, ** p<0.01, **** p<0.0001, ns=not significant.
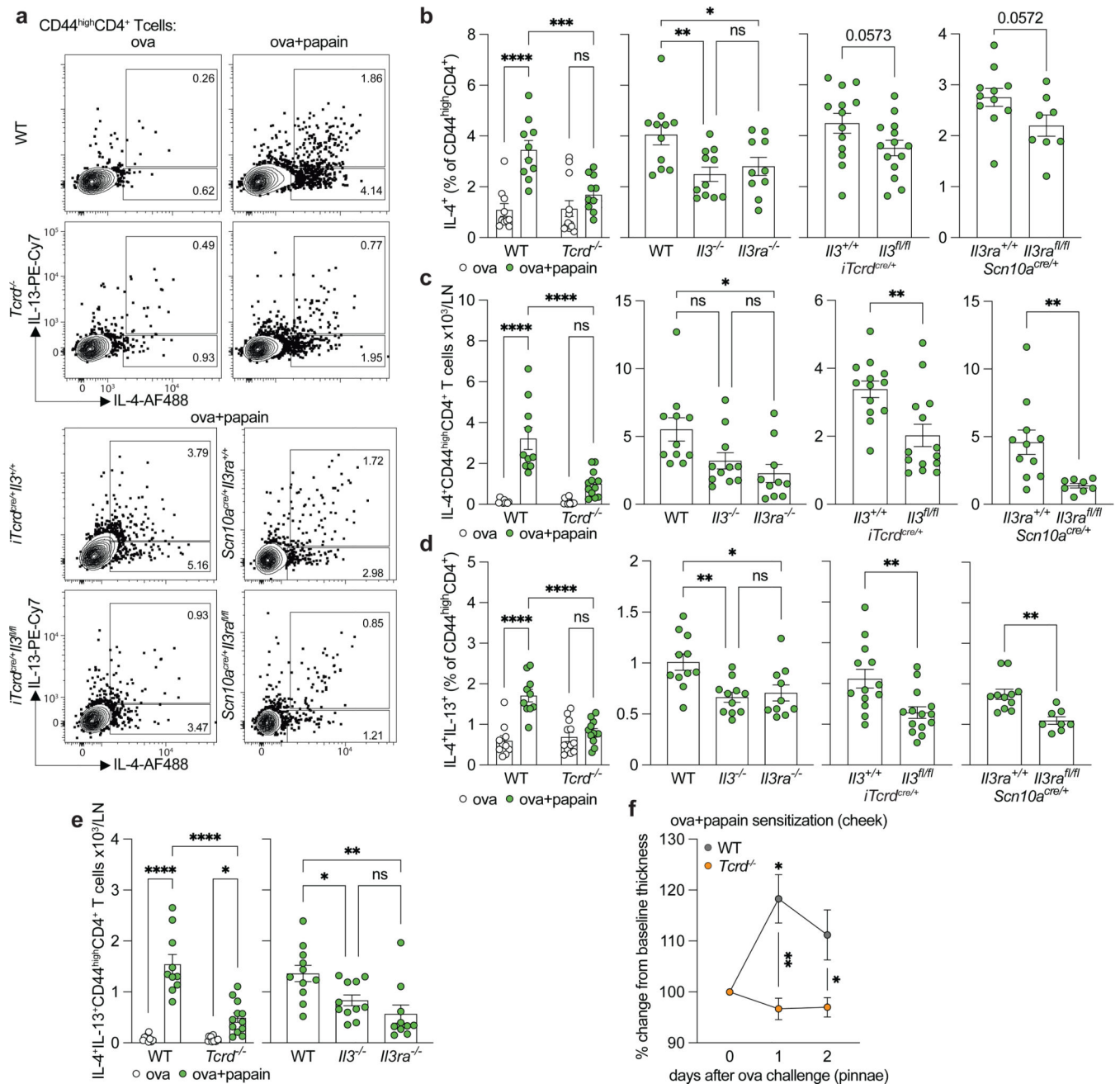
Extended Data Figure 9. The absence of the GD3-IL-3-sensory neuron axis impairs papain-induced Th2 differentiation.

a, Flow cytometry of the draining lymph node (dLN) 5 days after immunization with ova±papain (gating strategy corresponding to Figure 4c, j). **b-e**, Flow cytometric quantification of the draining lymph node (dLN) 5 days after immunization with ova±papain (n=10 WT; n=12 *Tcrd*$^{-/-}$; n=11 WT; n=11 *Il3*$^{-/-}$; n=10 *Il3ra*$^{-/-}$; n=13 *iTcrd*$^{cre/+}$*Il3*$^{+/+}$; n=14 *iTcrd*$^{cre/+}$*Il3*$^{fl/fl}$; n=11 *Scn10a*$^{cre/+}$*Il3ra*$^{+/+}$; n=8 *Scn10a*$^{cre/+}$*Il3ra*$^{fl/fl}$). **f**, Pinnae thickness after papain challenge following the induction of delayed-type hypersensitivity (n=10 WT; n=6 *Tcrd*$^{-/-}$). Symbols represent individual mice. Symbols connected by lines indicate paired samples. Bar plots and line graphs are mean ± SEM. Data represent at least two independent

experiments and were combined. Statistical tests: Two-way ANOVA with Tukey's multiple comparisons test (**b-d**; **e**, WT v *Tcrd*^{−/−}; **g**), Two-way repeated measures ANOVA (**i**), One-way ANOVA with Tukey's multiple comparisons test (**b-d**; **e**, WT v *Il3*^{−/−} v *Il3ra*^{−/−}), Two-sided unpaired *t*-test (**b-c**; **d**, *iTcrd*[cre/+] and *Scn10a*[cre/+]), or Two-sided Mann Whitney *U*-test (**e**). * p<0.05, ** p<0.01, *** p<0.001, **** p<0.0001, ns=not significant.
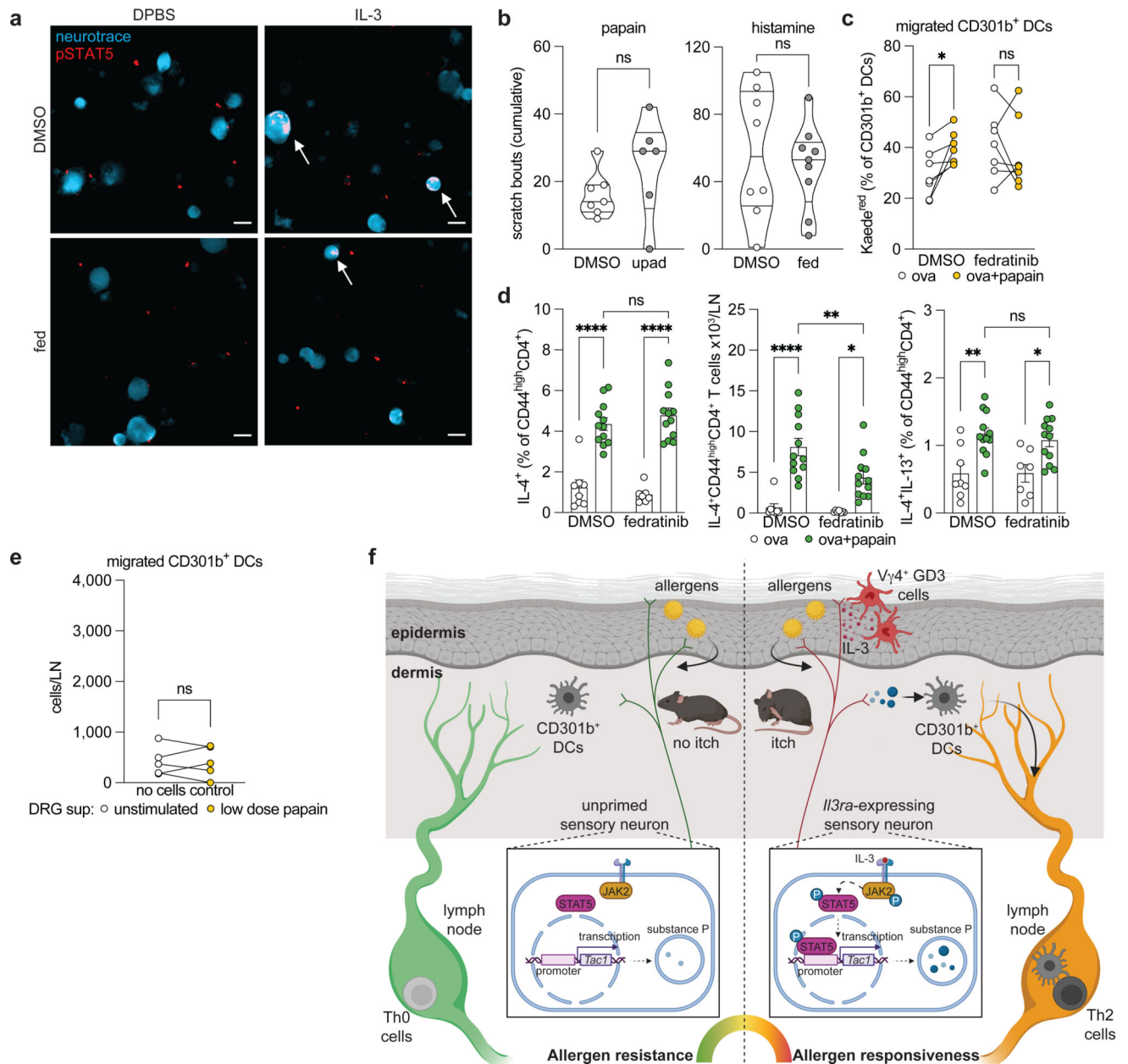
Extended Data Figure 10. Inhibition of the JAK2-STAT5 pathway reduces the responsiveness of sensory neurons to allergens.

a, Representative fluorescence microscopic images of pSTAT5 in DRG neurons. The scale bar is 20 μm. **b**, Cumulative cheek scratch bouts following i.d. injection of papain or histamine (papain: n=7 DMSO; n=6 upad; histamine: n=8 DMSO; n=9 fed). **c**, **e**, Flow

cytometric quantification of the draining lymph node (dLN) 24 hours after immunization as indicated (**c**: n=7 per group; **e**: n=5 per group). **d**, Flow cytometric quantification of the draining lymph node (dLN) 5 days after immunization with ova±papain (n=8 DMSO ova; n=12 DMSO ova+papain; n=7 fedratinib ova; n=12 fedratinib ova+papain). **f**, Graphical Abstract: a γδ T cell-IL-3 axis controls allergic responses through sensory neurons. Vγ4^{+} GD3 cells are the major source of IL-3 in naïve skin and control the allergen responsiveness of *Il3ra*-expressing sensory neurons. Upon allergen exposure, IL-3-primed sensory neurons respond with robust itch, Th2-skewing DC migration to the dLN, and Th2 differentiation in the dLN. Mechanistically, IL-3 activates JAK2 and STAT5, leading to the transcription of the substance P gene *Tac1*. While JAK2 is necessary for allergic itch and the initiation of the allergic immune response, STAT5 is only required for the initiation of the allergic immune response. Together, the GD3-IL-3 axis controls the initial sensory neuronal response to allergens, dictating whether an organism is resistant or sensitive to allergens. Symbols represent individual mice (**b**, **d**), while symbols connected by lines indicate paired samples (**c**, **e**). Violin plots show the median and quartiles. Bar plots are mean ± SEM. Data are representative of at least two experiments and combined. Statistical tests: Two-way repeated measures ANOVA (**c**, **e**), Two-way ANOVA with Tukey's multiple comparisons test (**d**), or Two-sided unpaired *t*-test (**b**). * p<0.05, ** p<0.01, **** p<0.0001, ns=not significant.

Supplementary Material

Refer to Web version on PubMed Central for supplementary material.

Acknowledgements

Competing interests

Data Availability

scRNAseq data generated in this project are deposited in the GEO database (under accession number GSE223220). scRNAseq from human skin[29,30] (https://vitiligo.dolphinnext.com/index.html, https://zenodo.org/record/4569496) and bulk RNAseq from mouse and human DRG[32] (https://www.ncbi.nlm.nih.gov/pmc/articles/PMC7305999/) were obtained from publically available sources. In the mouse scRNAseq experiment, raw sequencing data was aligned to the mouse reference genome (mm10, v2020-A from 10x Genomics). In the mouse scTCRseq experiment, raw sequencing data was aligned to the mouse immune repertoire genome (GRCm38, v7.0.0 from 10x Genomics). Source data are provided.

References

1. Perner C. et al. Substance P Release by Sensory Neurons Triggers Dendritic Cell Migration and Initiates the Type-2 Immune Response to Allergens. Immunity 53, 1063–1077.e1067, doi:10.1016/j.immuni.2020.10.001 (2020). [PubMed: 33098765]

2. Serhan N. et al. House dust mites activate nociceptor-mast cell clusters to drive type 2 skin inflammation. Nat Immunol 20, 1435–1443, doi:10.1038/s41590-019-0493-z (2019). [PubMed: 31591569]

3. Wilson SR et al. The epithelial cell-derived atopic dermatitis cytokine TSLP activates neurons to induce itch. Cell 155, 285–295, doi:10.1016/j.cell.2013.08.057 (2013). [PubMed: 24094650]

4. Voisin T. et al. The CysLT(2)R receptor mediates leukotriene C(4)-driven acute and chronic itch. Proc Natl Acad Sci U S A 118, doi:10.1073/pnas.2022087118 (2021).

5. Wang F. et al. A basophil-neuronal axis promotes itch. Cell 184, 422–440.e417, doi:10.1016/j.cell.2020.12.033 (2021). [PubMed: 33450207]

6. Cevikbas F. et al. A sensory neuron-expressed IL-31 receptor mediates T helper cell-dependent itch: Involvement of TRPV1 and TRPA1. J Allergy Clin Immunol 133, 448–460, doi:10.1016/j.jaci.2013.10.048 (2014). [PubMed: 24373353]

7. Oetjen LK et al. Sensory Neurons Co-opt Classical Immune Signaling Pathways to Mediate Chronic Itch. Cell 171, 217–228.e213, doi:10.1016/j.cell.2017.08.006 (2017). [PubMed: 28890086]

8. Castillo-González R, Cibrian D. & Sánchez-Madrid F. Dissecting the complexity of γδ T-cell subsets in skin homeostasis, inflammation, and malignancy. Journal of Allergy and Clinical Immunology 147, 2030–2042, doi:10.1016/j.jaci.2020.11.023 (2021). [PubMed: 33259837]

9. Hoeffel G. et al. Sensory neuron-derived TAFA4 promotes macrophage tissue repair functions. Nature 594, 94–99, doi:10.1038/s41586-021-03563-7 (2021). [PubMed: 34012116]

10. Chiu IM et al. Bacteria activate sensory neurons that modulate pain and inflammation. Nature 501, 52–57, doi:10.1038/nature12479 (2013). [PubMed: 23965627]

11. Riol-Blanco L. et al. Nociceptive sensory neurons drive interleukin-23-mediated psoriasiform skin inflammation. Nature 510, 157–161, doi:10.1038/nature13199 (2014). [PubMed: 24759321]

12. Kumamoto Y. et al. CD301b+ dermal dendritic cells drive T helper 2 cell-mediated immunity. Immunity 39, 733–743, doi:10.1016/j.immuni.2013.08.029 (2013). [PubMed: 24076051]

13. Sokol CL, Barton GM, Farr AG & Medzhitov R. A mechanism for the initiation of allergen-induced T helper type 2 responses. Nat Immunol 9, 310–318, doi:10.1038/ni1558 (2008). [PubMed: 18300366]

14. Shimada SG & LaMotte RH Behavioral differentiation between itch and pain in mouse. Pain 139, 681–687, doi:10.1016/j.pain.2008.08.002 (2008). [PubMed: 18789837]

15. Meixiong J. et al. Activation of Mast-Cell-Expressed Mas-Related G-Protein-Coupled Receptors Drives Non-histaminergic Itch. Immunity 50, 1163–1171.e1165, doi:10.1016/j.immuni.2019.03.013 (2019). [PubMed: 31027996]

16. Nielsen MM, Witherden DA & Havran WL γδ T cells in homeostasis and host defence of epithelial barrier tissues. Nature Reviews Immunology 17, 733–745, doi:10.1038/nri.2017.101 (2017).

17. Boyden LM et al. Skint1, the prototype of a newly identified immunoglobulin superfamily gene cluster, positively selects epidermal gammadelta T cells. Nat Genet 40, 656–662, doi:10.1038/ng.108 (2008). [PubMed: 18408721]

18. Havran WL et al. Limited diversity of T-cell receptor gamma-chain expression of murine Thy-1+ dendritic epidermal cells revealed by V gamma 3-specific monoclonal antibody. Proc Natl Acad Sci U S A 86, 4185–4189, doi:10.1073/pnas.86.11.4185 (1989). [PubMed: 2726770]

19. Nielsen MM et al. IL-1β–Dependent Activation of Dendritic Epidermal T Cells in Contact Hypersensitivity. The Journal of Immunology 192, 2975–2983, doi:10.4049/jimmunol.1301689 (2014). [PubMed: 24600030]

20. Chodaczek G, Papanna V, Zal MA & Zal T. Body-barrier surveillance by epidermal γδ TCRs. Nature Immunology 13, 272–282, doi:10.1038/ni.2240 (2012). [PubMed: 22327568]

21. Tan L. et al. Single-Cell Transcriptomics Identifies the Adaptation of Scart1+ Vγ6+ T Cells to Skin Residency as Activated Effector Cells. Cell Reports 27, 3657–3671.e3654, doi:10.1016/j.celrep.2019.05.064 (2019). [PubMed: 31216482]

22. McKenzie DR et al. Normality sensing licenses local T cells for innate-like tissue surveillance. Nature Immunology 23, 411–422, doi:10.1038/s41590-021-01124-8 (2022). [PubMed: 35165446]

23. Russell-Goldman E. & Murphy GF The Pathobiology of Skin Aging: New Insights into an Old Dilemma. The American Journal of Pathology 190, 1356–1369, doi:10.1016/j.ajpath.2020.03.007 (2020). [PubMed: 32246919]

24. Naik S. et al. Compartmentalized control of skin immunity by resident commensals. Science 337, 1115–1119, doi:10.1126/science.1225152 (2012). [PubMed: 22837383]

25. Augustin M. et al. Prevalence, predictors and comorbidity of dry skin in the general population. Journal of the European Academy of Dermatology and Venereology 33, 147–150, doi:10.1111/jdv.15157 (2019). [PubMed: 29953684]

26. Wärnberg Gerdin S. et al. Impaired skin barrier and allergic sensitization in early infancy. Allergy 77, 1464–1476, doi:10.1111/all.15170 (2022). [PubMed: 34738238]

27. Gentek R. et al. Epidermal γδ T cells originate from yolk sac hematopoiesis and clonally self-renew in the adult. Journal of Experimental Medicine 215, 2994–3005, doi:10.1084/jem.20181206 (2018). [PubMed: 30409784]

28. Mohamed RH et al. The SKINT1-Like Gene Is Inactivated in Hominoids But Not in All Primate Species: Implications for the Origin of Dendritic Epidermal T Cells. PLOS ONE 10, e0123258, doi:10.1371/journal.pone.0123258 (2015).

29. Gellatly KJ et al. scRNA-seq of human vitiligo reveals complex networks of subclinical immune activation and a role for CCR5 in T(reg) function. Sci Transl Med 13, eabd8995, doi:10.1126/scitranslmed.abd8995 (2021).

30. Reynolds G. et al. Developmental cell programs are co-opted in inflammatory skin disease. Science 371, doi:10.1126/science.aba6500 (2021).

31. Dougan M, Dranoff G. & Dougan SK GM-CSF, IL-3, and IL-5 Family of Cytokines: Regulators of Inflammation. Immunity 50, 796–811, doi:10.1016/j.immuni.2019.03.022 (2019). [PubMed: 30995500]

32. Wangzhou A. et al. Pharmacological target-focused transcriptomic analysis of native vs cultured human and mouse dorsal root ganglia. Pain 161, 1497–1517, doi:10.1097/j.pain.0000000000001866 (2020). [PubMed: 32197039]

33. Jung M. et al. Cross-species transcriptomic atlas of dorsal root ganglia reveals species-specific programs for sensory function. Nat Commun 14, 366, doi:10.1038/s41467-023-36014-0 (2023). [PubMed: 36690629]

34. Sharma N. et al. The emergence of transcriptional identity in somatosensory neurons. Nature 577, 392–398, doi:10.1038/s41586-019-1900-1 (2020). [PubMed: 31915380]

35. Zeisel A. et al. Molecular Architecture of the Mouse Nervous System. Cell 174, 999–1014.e1022, doi:10.1016/j.cell.2018.06.021 (2018). [PubMed: 30096314]

36. Usoskin D. et al. Unbiased classification of sensory neuron types by large-scale single-cell RNA sequencing. Nature Neuroscience 18, 145–153, doi:10.1038/nn.3881 (2015). [PubMed: 25420068]

37. Silverberg JI et al. Efficacy and Safety of Abrocitinib in Patients With Moderate-to-Severe Atopic Dermatitis: A Randomized Clinical Trial. JAMA Dermatology 156, 863–873, doi:10.1001/jamadermatol.2020.1406 (2020). [PubMed: 32492087]

38. Narla S, Silverberg JI & Simpson EL Management of inadequate response and adverse effects to dupilumab in atopic dermatitis. Journal of the American Academy of Dermatology 86, 628–636, doi:10.1016/j.jaad.2021.06.017 (2022). [PubMed: 34126094]

39. Toulon A. et al. A role for human skin–resident T cells in wound healing. Journal of Experimental Medicine 206, 743–750, doi:10.1084/jem.20081787 (2009). [PubMed: 19307328]

40. Profet M. The Function of Allergy: Immunological Defense Against Toxins. The Quarterly Review of Biology 66, 23–62 (1991). [PubMed: 2052671]

41. McAlpine CS et al. Astrocytic interleukin-3 programs microglia and limits Alzheimer's disease. Nature 595, 701–706, doi:10.1038/s41586-021-03734-6 (2021). [PubMed: 34262178]

42. Kiss MG et al. Interleukin-3 coordinates glial-peripheral immune crosstalk to incite multiple sclerosis. Immunity 56, 1502–1514.e1508, doi:10.1016/j.immuni.2023.04.013 (2023). [PubMed: 37160117]

43. Lefteri DA et al. Mosquito saliva enhances virus infection through sialokinin-dependent vascular leakage. Proc Natl Acad Sci U S A 119, e2114309119, doi:10.1073/pnas.2114309119 (2022).

44. Sandrock I. et al. Genetic models reveal origin, persistence and non-redundant functions of IL-17-producing γδ T cells. J Exp Med 215, 3006–3018, doi:10.1084/jem.20181439 (2018). [PubMed: 30455268]

45. Zhang B. et al. Differential Requirements of TCR Signaling in Homeostatic Maintenance and Function of Dendritic Epidermal T Cells. J Immunol 195, 4282–4291, doi:10.4049/jimmunol.1501220 (2015). [PubMed: 26408667]

46. Voehringer D, Liang HE & Locksley RM Homeostasis and effector function of lymphopenia-induced "memory-like" T cells in constitutively T cell-depleted mice. J Immunol 180, 4742–4753, doi:10.4049/jimmunol.180.7.4742 (2008). [PubMed: 18354198]

47. Miyamoto T, Nojima H, Shinkado T, Nakahashi T. & Kuraishi Y. Itch-Associated Response Induced by Experimental Dry Skin in Mice. Japanese Journal of Pharmacology 88, 285–292, doi:10.1254/jjp.88.285 (2002). [PubMed: 11949883]

48. Trier AM et al. IL-33 signaling in sensory neurons promotes dry skin itch. J Allergy Clin Immunol 149, 1473–1480.e1476, doi:10.1016/j.jaci.2021.09.014 (2022). [PubMed: 34560104]

49. Yarmolinsky DA et al. Coding and Plasticity in the Mammalian Thermosensory System. Neuron 92, 1079–1092, doi:10.1016/j.neuron.2016.10.021 (2016). [PubMed: 27840000]

50. Thévenaz P, Ruttimann UE & Unser M. A pyramid approach to subpixel registration based on intensity. IEEE Trans Image Process 7, 27–41, doi:10.1109/83.650848 (1998). [PubMed: 18267377]

51. Pnevmatikakis Eftychios A. et al. Simultaneous Denoising, Deconvolution, and Demixing of Calcium Imaging Data. Neuron 89, 285–299, doi:10.1016/j.neuron.2015.11.037 (2016). [PubMed: 26774160]

52. Roth BL DREADDs for Neuroscientists. Neuron 89, 683–694, doi:10.1016/j.neuron.2016.01.040 (2016). [PubMed: 26889809]

53. Tomura M. et al. Monitoring cellular movement in vivo with photoconvertible fluorescence protein "Kaede" transgenic mice. Proceedings of the National Academy of Sciences 105, 10871–10876, doi:doi:10.1073/pnas.0802278105 (2008).

54. Lee M. et al. Single-cell RNA sequencing identifies shared differentiation paths of mouse thymic innate T cells. Nature Communications 11, 4367, doi:10.1038/s41467-020-18155-8 (2020).

55. Zheng GX et al. Massively parallel digital transcriptional profiling of single cells. Nat Commun 8, 14049, doi:10.1038/ncomms14049 (2017). [PubMed: 28091601]

56. Li B. et al. Cumulus provides cloud-based data analysis for large-scale single-cell and single-nucleus RNA-seq. Nat Methods 17, 793–798, doi:10.1038/s41592-020-0905-x (2020). [PubMed: 32719530]

57. Batson J, Royer L. & Webber J. Molecular Cross-Validation for Single-Cell RNA-seq. bioRxiv, 786269, doi:10.1101/786269 (2019).

58. La Manno G. et al. RNA velocity of single cells. Nature 560, 494–498, doi:10.1038/ s41586-018-0414-6 (2018). [PubMed: 30089906]

59. Bergen V, Lange M, Peidli S, Wolf FA & Theis FJ Generalizing RNA velocity to transient cell states through dynamical modeling. Nature Biotechnology 38, 1408–1414, doi:10.1038/ s41587-020-0591-3 (2020).

60. Lange M. et al. CellRank for directed single-cell fate mapping. Nature Methods 19, 159–170, doi:10.1038/s41592-021-01346-6 (2022). [PubMed: 35027767]
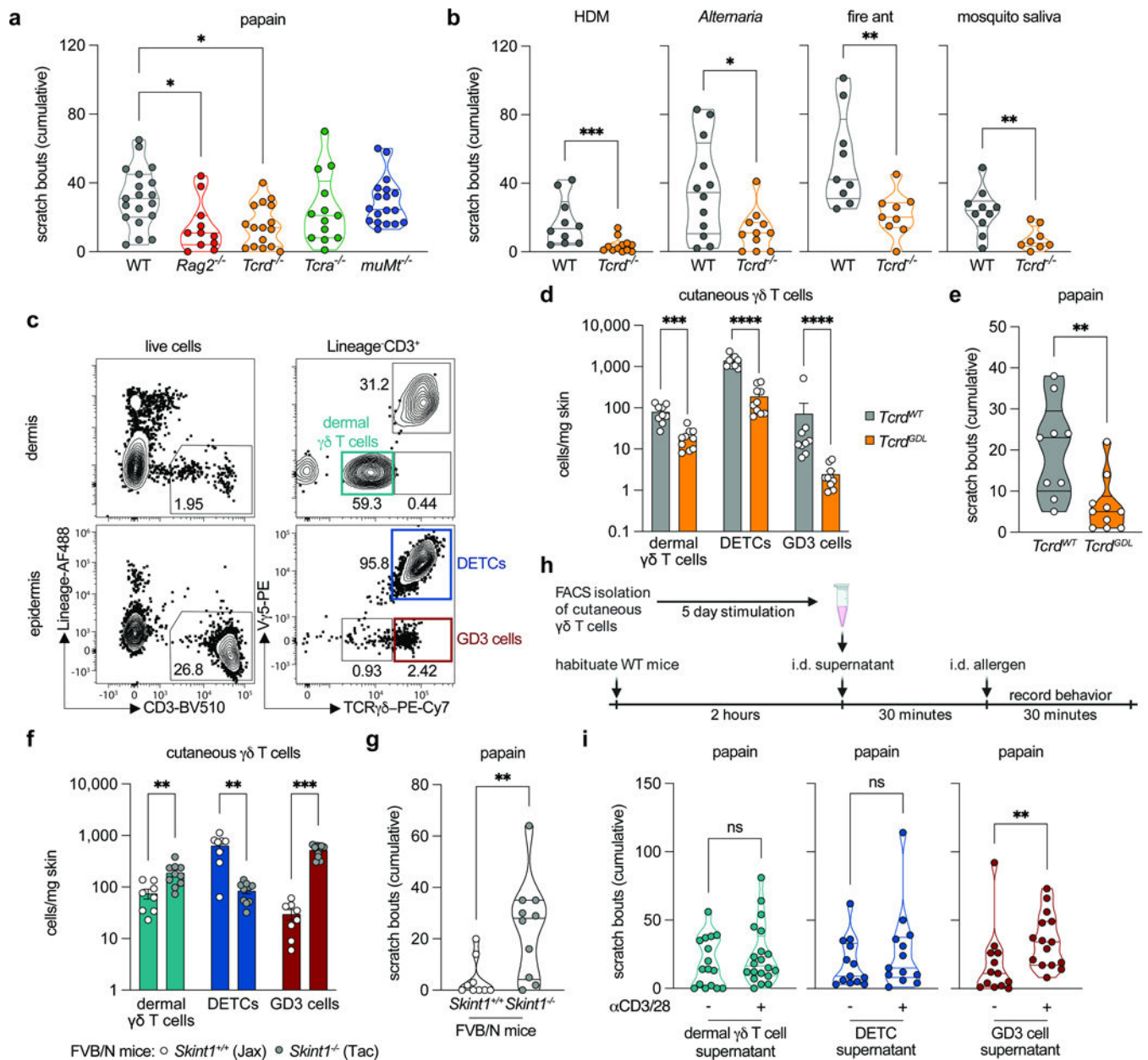
Figure 1. γδ T cells promote allergic itch through a secreted factor.

a, Cumulative cheek scratch bouts following intradermal (i.d.) injection with papain [n=19 WT (C57BL/6); n=11 *Rag2*^{−/−}; n=16 *Tcrd*^{−/−}; n=13 *Tcra*^{−/−}; n=18 *muMT*^{−/−}]. **b**, Cumulative cheek scratch bouts following i.d. injection with HDM (n=10 WT; n=12 *Tcrd*^{−/−}), *Alternaria* (n=12 WT; n=11 *Tcrd*^{−/−}), fire ant (n=9 per group), or mosquito saliva (n=10 WT; n=8 *Tcrd*^{−/−}). **c**, Flow cytometry of dermis or epidermis, from naïve WT pinnae. **d**, **f**, Flow cytometric quantification of skin (dermis+epidermis) γδ T cells from pinnae (n=9 *Tcrd*[WT]; n=10 *Tcrd*[GDL]; n=8 *Skint1*^{+/+}; n=10 *Skint1*^{−/−}). **e**, **g**, Cumulative cheek scratch bouts following i.d. injection with papain (n=9 *Tcrd*[WT]; n=10 *Tcrd*[GDL]; n=9 *Skint1*^{+/+}; n=10 *Skint1*^{−/−}). **h**, Schematic of γδ T cell supernatant transfer and behavior protocol. **i**, Cumulative cheek scratch bouts following i.d. injection of γδ T supernatant, then papain

(n=16 dermal γδ T cell unstimulated; n=20 dermal γδ T cell αCD3/28; n=13 DETC unstimulated, DETC αCD3/28, or GD3 unstimulated; n=15 GD3 αCD3/28). Symbols represent individual mice. Violin plots show the median and quartiles. Bar plots are mean ± SEM. Data represent at least two independent experiments and were combined. Statistical tests: Ordinary One-way ANOVA with Tukey's multiple comparisons test (**a**), Two-sided unpaired *t*-test (**b**: *Alternaria*, fire ant, mosquito saliva), or Two-sided Mann Whitney *U*-test (**b**: HDM, **d-g**, **i**). * p<0.05, ** p<0.01, *** p<0.001, **** p<0.0001, ns=not significant.
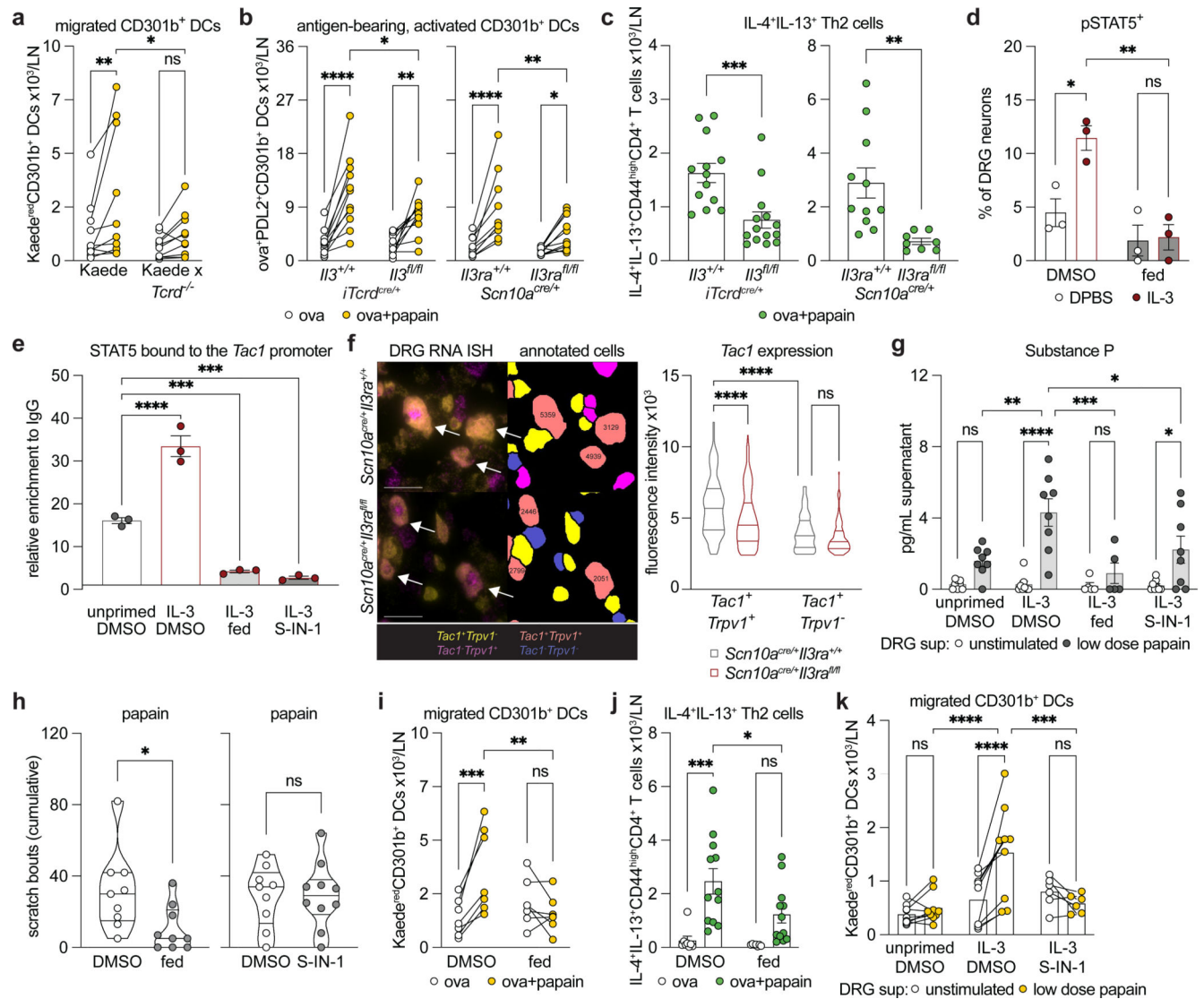
Figure 2. GD3 cells are required for allergic itch, associated with sensory neurons, and transcriptionally related to human epidermal T cells.

a, Uniform manifold approximation and projection (UMAP) plot of naïve WT pinnae γδ T cells analyzed by scRNAseq. **b**, Bubble plot of *Trgv* and *Trdv* genes in clones of GD3 cells analyzed by scTCRseq (size denoting the percentage of GD3 cells expressing a *Trdv* gene pair; color denoting the percentage of cells with a given *Trdv* gene that has the given *Trgv* gene). **c**, Flow cytometry of naïve WT pinnae. FMO=fluorescence minus one. **d**, Cumulative cheek scratch bouts following i.d. injection with papain (left panel; n=16 WT; n=10 *Trgv4*^{−/−}). Flow cytometry of naïve pinnae (right panel; n=11 per group). **e**, Confocal microscopy z-stack of naïve *Scn10a*[tdTomato] pinnae. The scale bar is 10 μm. **f**, Orthoganol depiction of the x, y, and z planes of the z-stack in **e**. Arrows show the same location in x, y, and z space. **g**, UMAP plot of healthy human epidermal cells re-clustered from the Gellatly et al.[29] publicly available dataset. **h**, Heatmap (z-score) of the human homologs of the top 25 differentially expressed mouse GD3 cell genes compared to dermal γδ T cells. **i**, Heatmap of the enrichment scores from gene set enrichment analysis comparing the genes in **h** to the

human clusters from **g**. p<0.05 is shown. **j**, UMAP plot of the z-score of the genes from **h**. Symbols represent individual mice. Violin plots show the median and quartiles. Bar plots are the mean. Mouse data represent at least two independent experiments (**c-f**), combined in **d**. Statistical tests: Two-sided Mann Whitney *U*-test (**d**). * p<0.05.
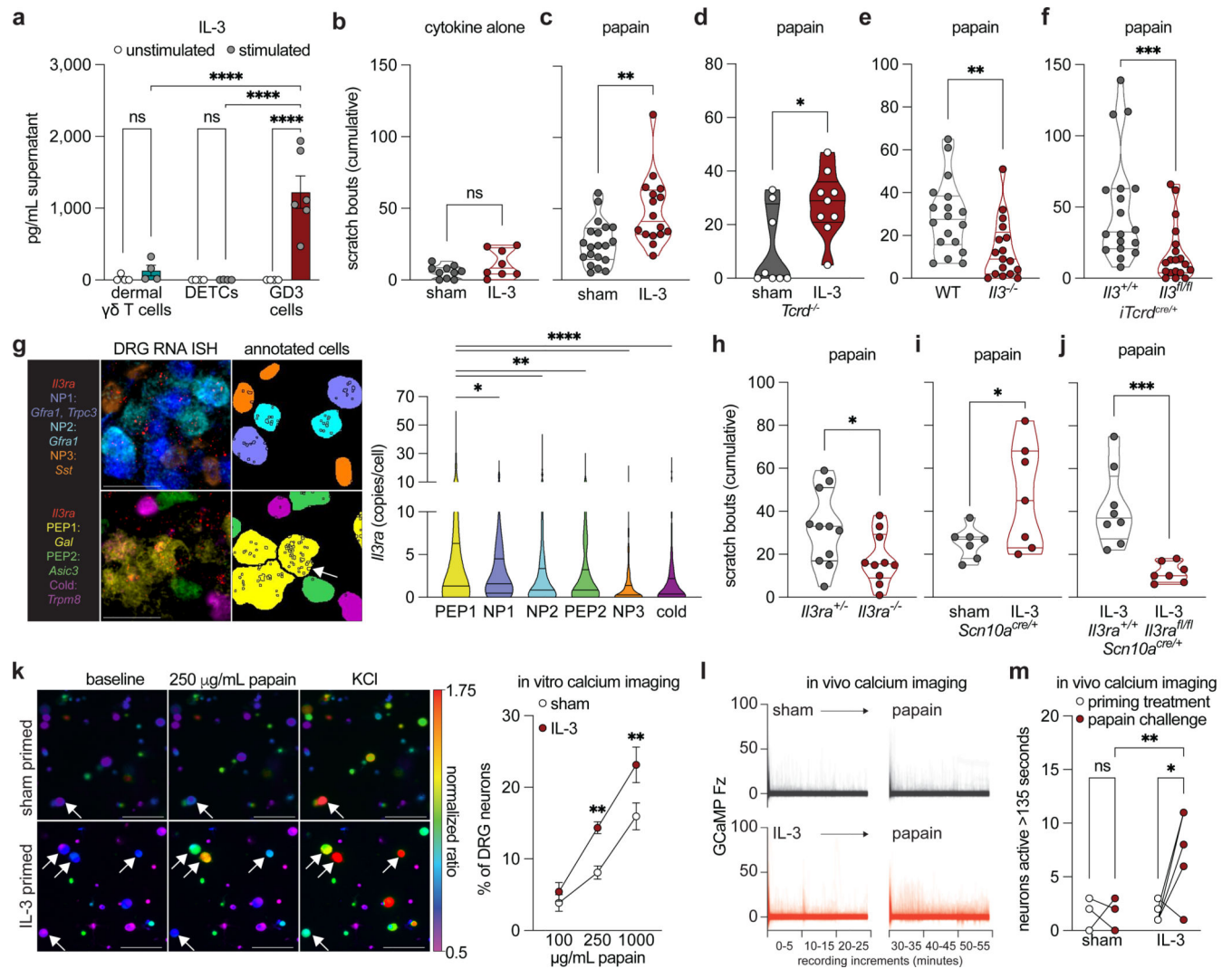
Figure 3. GD3 cell IL-3 primes the allergen responsiveness of sensory neurons through *Il3ra*.
a, IL-3 ELISA of cell-free supernatant from FACS isolated γδ T cells stimulated as indicated [n=4 per group, except for stimulated GD3 cells (n=6)]. **b-d**, **i-j**, Cumulative cheek scratch bouts following i.d. injection of IL-3 (**b**: n=10 sham; n=8 IL-3), then papain (**c**: n=20 sham; n=16 IL-3; **d**: n=8 sham; n=9 IL-3; **i**: n=7 per group; **j**: n=8 *Scn10a^cre/+^Il3ra^+/+^*; n=7 *Scn10a^cre/+^Il3ra^fl/fl^*) in WT (**b-c**), *Tcrd^-/-^* (**d**), or *Scn10a^cre/+^* (**i-j**) mice. **e-f**, **h**, Cumulative cheek scratch bouts following i.d. injection of papain (**e**: n=18 WT; n=17 *Il3^-/-^*; **f**: n=18 *iTcrd^cre/+^Il3^+/+^*; n=19 *iTcrd^cre/+^Il3^fl/fl^*; **h**: n=11 *Il3ra^+/-^*; n=10 *Il3ra^-/-^*). **g**, RNA fluorescence *in situ* hybridization (RNA ISH) of mouse DRG tissue sections. The arrow indicates a cell with *Il3ra* expression (open circles). The scale bar indicates 50 μm (n=134 PEP1; n=114 NP1; n=139 NP2; n=256 NP2; n=192 NP3; n=152 cold). **k**, Ratiometric calcium imaging of DRG neurons stimulated with papain. Arrows show neurons excited by 250 μg/mL papain. The scale bar indicates 20 μm (n=11 sham; n=10 IL-3). **l-m**, GCaMP imaging of trigeminal ganglia neurons from mice i.d. immunized with sham DPBS or IL-3, then papain (n=4 sham; n=5 IL-3). Symbols represent individual wells (**a**), mice (**b-f**, **h-j**, **m**), or mean ± SEM of experiments (**k**). Bar and dose-response plots are mean ±

SEM. Violin plots show the median and quartiles. Data represent at least two independent experiments and were combined, except in **a**. Statistical tests: Two-way ANOVA with Tukey's multiple comparisons test (**a**), Two-way repeated measures ANOVA with Tukey's multiple comparisons test (**k**), Two-way repeated measures ANOVA (**m**), One-way ANOVA with Tukey's multiple comparisons test (**g**), Two-sided unpaired *t*-test (**b, h-j**), or Two-sided Mann Whitney *U*-test (**c-f**). * $p < 0.05$, ** $p < 0.01$, *** $p < 0.001$, ns=not significant.
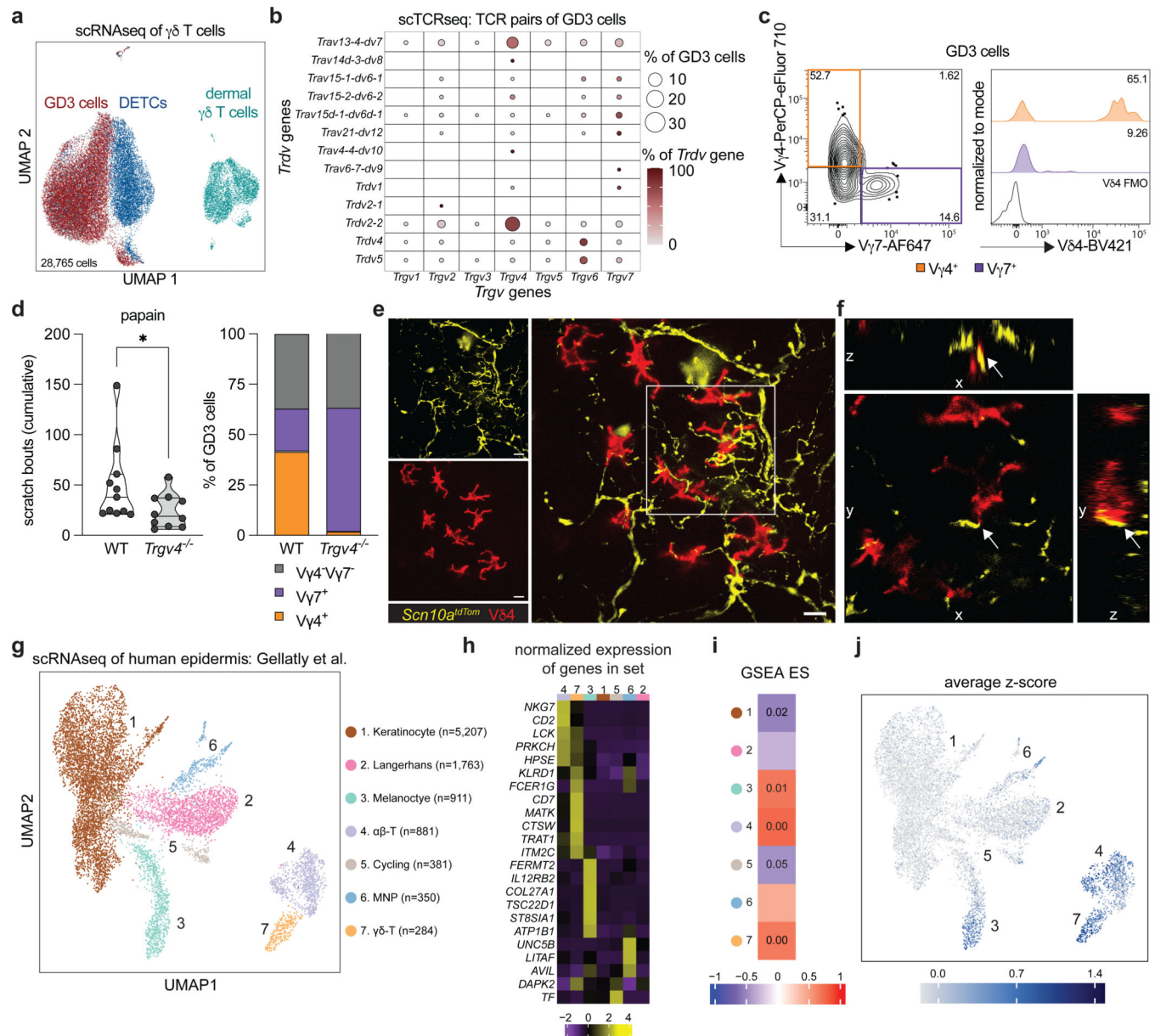
Figure 4. Distinct IL-3-induced JAK2/STAT5 mechanisms underlie sensory neuronal responsiveness to allergens.

a-b, **i**, **k**, Flow cytometric quantification of CD301b⁺ DCs per dLN that migrated from photoconverted (Kaede^red) skin (**a**, **i**, **k**) or were activated and antigen-bearing (**b**) after immunization as indicated (**a**: n=10 per group; **b**: n=11 per group, except for *Scn10a^cre/+Il3ra^+/+* (n=10); **i**: n=7 per group; **k**: n=9 per group, except IL-3 S-IN-1 (n=6)]. **c, j,** Flow cytometric quantification of IL-4⁺IL-13⁺CD44^highCD4⁺ T cells in the dLN after immunization as indicated (**c**: n=13 *iTcrd^cre/+Il3^+/+*; n=14 *iTcrd^cre/+Il3^fl/fl*; n=11 *Scn10a^cre/+Il3ra^+/+*; n=8 *Scn10a^cre/+Il3ra^fl/fl*; **j**: n=8 DMSO/ova; n=12 ova+papain; n=7 fed/ova). **d**, Fluorescence microscopy of pSTAT5 in DRG neurons (n=3 per group). **e**, Chromatin immunoprecipitation of STAT5 associated with the *Tac1* promoter of DRG neurons (n=3 per group). **f**, RNA ISH of mouse DRG tissue sections. The arrow indicates a *Tac1⁺Trpv1⁺* cell.

The scale bar indicates 50 μm (n=141 $Tac1^+Trpv1^+ Scn10a^{cre/+}Il3ra^{+/+}$; n=61 $Tac1^+Trpv1^- Scn10a^{cre/+}Il3ra^{+/+}$; n=172 $Tac1^+Trpv1^+ Scn10a^{cre/+}Il3ra^{fl/fl}$; n=106 $Tac1^+Trpv1^- Scn10a^{cre/+}Il3ra^{fl/fl}$). **g**, Substance P ELISA of cell-free supernatant from DRG neurons stimulated as indicated [n=8 per group, except IL-3/fed (n=5)]. **h**, Cumulative cheek scratch bouts following i.d. injection of papain [n=9 per group, except S-IN-1 (n=10)]. Symbols represent individual mice (**c**, **h**, **j**), experimental replicates (**d**), individual wells (**e**), or paired samples (**a-b**, **i-k**). Bar plots are mean ± SEM. Violin plots show the median and quartiles. Data represent at least two independent experiments and were combined, except in (**e**) where one representative experiment is shown. Statistical tests: Two-way repeated measures ANOVA (**a-b**, **i-k**), Two-way ANOVA with Tukey's multiple comparisons test (**d**, **f-g**, **j**), One-way ANOVA with Tukey's multiple comparisons test (**e**), Two-sided unpaired t-test (**c**; **h**, DMSO v S-IN-1), or Two-sided Mann Whitney U-test (**h**, DMSO v fed). * $p<0.05$, ** $p<0.01$, *** $p<0.001$, **** $p<0.0001$, ns=not significant.